





15 Abstract

16 The assessment of cropland carbon and nitrogen (C & N) balances play a key role to identify  
17 cost effective mitigation measures to combat climate change and reduce environmental  
18 pollution. In this paper, a biogeochemical modelling approach is adopted to assess all C & N  
19 fluxes in a regional cropland ecosystem of Thessaly, Greece. Additionally, the estimation and  
20 quantification of the modelling uncertainty in the regional inventory are realized through the  
21 propagation of parameter distributions through the model leading to result distributions for  
22 modelling estimations. The model was applied on a regional dataset of approximately 1000  
23 polygons deploying model initializations and crop rotations for the 5 major crop cultivations  
24 and for a timespan of 8 years. The full statistical analysis on modelling results yields for the C  
25 balance carbon input fluxes into the soil of  $12.4 \pm 1.4$  tons C ha<sup>-1</sup> yr<sup>-1</sup> and output fluxes of  $11.9$   
26  $\pm 1.3$  tons C ha<sup>-1</sup> yr<sup>-1</sup>, with a resulting average carbon sequestration of  $0.5 \pm 0.3$  tons C ha<sup>-1</sup> yr<sup>-1</sup>.  
27 The averaged N influx was  $212.3 \pm 9.1$  kg N ha<sup>-1</sup> yr<sup>-1</sup> while outfluxes were estimated on  
28 average of  $198.3 \pm 11.2$  kg N ha<sup>-1</sup> yr<sup>-1</sup>. The net N accumulation into the soil nitrogen pools was  
29 estimated to  $14.0 \pm 2.1$  kg N ha<sup>-1</sup> yr<sup>-1</sup>. The N outflux consist of gaseous N fluxes composed by  
30 N<sub>2</sub>O emissions  $2.6 \pm 0.8$  kg N<sub>2</sub>O-N ha<sup>-1</sup> yr<sup>-1</sup>, NO emissions of  $3.2 \pm 1.5$  kg NO-N ha<sup>-1</sup> yr<sup>-1</sup>, N<sub>2</sub>  
31 emissions  $15.5 \pm 7.0$  kg N<sub>2</sub>-N ha<sup>-1</sup> yr<sup>-1</sup> and NH<sub>3</sub> emissions of  $34.0 \pm 6.7$  kg NH<sub>3</sub>-N ha<sup>-1</sup> yr<sup>-1</sup>, as  
32 well as aquatic N fluxes (only nitrate leaching into surface waters) of  $14.1 \pm 4.5$  kg NO<sub>3</sub>-N ha<sup>-1</sup>  
33 yr<sup>-1</sup>, N fluxes of N removed from the fields in yields, straw and feed of  $128.8 \pm 8.5$  kg N ha<sup>-1</sup> yr<sup>-1</sup>.  
34 1.

35

36 KEYWORDS: climate change mitigation, greenhouse emissions, ecosystem modelling,  
37 cropland carbon and nitrogen balance, inventory, Thessaly region, LandscapeDNDC

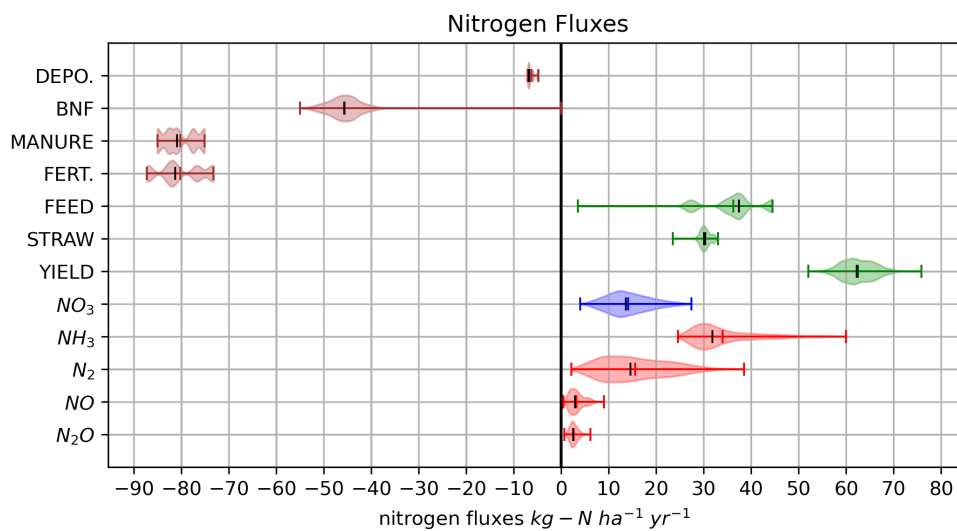
38

39



40 Graphical abstract: Result distributions of all nitrogen fluxes with means and medians

41



42

43



44 1 Introduction

45 Food security as well as the agricultural productivity depend to a major extend on the applied  
46 nitrogen (N) fertilizers (Klatt et al., 2015a). Worldwide, the N fertilizer use for the years 1960 to  
47 2005 has increased from 30 to 154 million tons (IFADATA, 2015). In Europe, the increase of  
48 yields in arable land and grassland systems was 45-70% since 1950 (EFMA, 2009) due to the  
49 agricultural production systems intensification. Excessive use of N fertilizers, though  
50 beneficially affecting the yield, could cause a harmful impact to the environment, e.g. increased  
51 gaseous emissions and aquatic fluxes of nitrous oxide (N<sub>2</sub>O) to the atmosphere and leaching  
52 of nitrate (NO<sub>3</sub>) into water bodies (Erisman et al., 2011; Galloway et al., 2013; Kim et al., 2015)  
53 The N<sub>2</sub>O poses a twofold environmental threat. From the one hand, it is a strong greenhouse  
54 gas with a warming potential of 300 times greater (in a 100-year time period) than carbon  
55 dioxide (CO<sub>2</sub>) and from the other hand, it is a major driver of ozone depletion in stratosphere  
56 (Ravishankara et al., 2009). The fertilizer use aiming at the increase of the agricultural  
57 production is the most crucial anthropogenic source of atmospheric N<sub>2</sub>O, which at present  
58 contributes for approximately 45% of total anthropogenic N<sub>2</sub>O emissions on a global scale  
59 (Jones et al., 2014). Because of the global population growth and thus a growing food and  
60 feed demand (Godfray et al., 2010), the fertilizer use will probably increase. Consequently, the  
61 prediction of the current business-as-usual scenarios show doubled anthropogenic N<sub>2</sub>O  
62 emissions by the year 2050 (Davidson and Kanter, 2014). The European countries have  
63 recently set up bilateral agreements in order to reduce N<sub>2</sub>O emissions from cultivated crop  
64 lands (EU-Commission, 2014). Similarly, the European Nitrates Directive (EU-Commission,  
65 2019; Musacchio et al., 2020) aims at NO<sub>3</sub> leaching reduction to water bodies to avoid both an  
66 increase of eutrophication (Camargo and Alonso, 2006) and drinking water pollution. Because  
67 of the hazardous N<sub>2</sub>O and NO<sub>3</sub> effects, agricultural systems are necessary to be evaluated for  
68 their profitability and productivity as well as for their impacts to the environment.

69 The N<sub>2</sub>O and NO<sub>3</sub> production and consumption in agricultural lands are regulated to a large  
70 extend by N plant uptake and, also, the microbial processes of denitrification and nitrification  
71 (Butterbach-Bahl et al., 2013). The factors controlling both the microbial metabolism and plant



72 N uptake are a) soil conditions (Butterbach-Bahl et al., 2013) and b) cultivation management  
73 practices e.g. crop rotation, fertilizing amount and timing, and ploughing (Smith et al., 2008).  
74 In order to reach a minimization of the environmental footprint of feed and agricultural  
75 production while securing the global food security (Garnett et al., 2013), it is mandatory to  
76 tighten the N cycling on intensified agricultural systems e.g., by harmonizing N demand of  
77 crops with soil N availability driven by fertilization.

78 A number of environmental/ecosystem models have been developed and used to describe the  
79 structure of multiple biogeochemical processes (Wainwright and Mulligan, 2004.). For the  
80 estimation/quantification of the GHGs emissions from different agroecosystems, modelling  
81 approaches are constantly gaining ground due to the in-situ data limitation (field campaign and  
82 laboratory costs) and the variation in spatial and temporal scales. The simulated results may,  
83 also, have uncertainties resulting from different sources, which can be, though, quantified  
84 increasing the accuracy of the estimates. Mechanistic models integrating relevant processes,  
85 which simulate agricultural production, and, also, reactive N losses to the environment are  
86 valuable tools to infer practices for a sustainable agriculture. In recent years, process-based  
87 biogeochemical models such as e.g. DNDC (Li, 2000), DAYCENT (Parton et al., 1998),  
88 ECOSSE (Bell et al., 2012) and CERES-EGC (Gabrielle et al., 2006) have proven their  
89 applicability to simulate N<sub>2</sub>O emissions and NO<sub>3</sub> leaching from various land uses. Despite the  
90 fact that their accuracy is being assessed against in-situ data, few studies are reported to use  
91 sensitivity and uncertainty analyses in total N and C cycling simulation by process-based  
92 models (Verbeeck et al., 2006).

93 In this analysis, the process-based bio-geochemical model LandscapeDNDC (Haas et al.,  
94 2013) was applied to the agricultural cropland systems in the region of Thessaly (Greece). The  
95 objective of our study was to i) assess and report the cropland C and N balance including all  
96 associated fluxes such as e.g. CO<sub>2</sub>, N<sub>2</sub>O and NH<sub>3</sub> emissions, NO<sub>3</sub> leaching as well as the soil  
97 carbon stock changes; ii) to assess and quantify the modelling uncertainty of the simulated C  
98 and N balance and flux estimations as requested by the IPCC (IPCC, 2019); and iii) to  
99 demonstrate the feasibility and robustness of a regional uncertainty assessment methodology



100 for C and N cycling by propagating 500 joint parameter and input data distributions through  
101 the model (each representing a full regional inventory simulation) yielding regional result  
102 distributions for any modelling estimations.

103

## 104 2 Material and Methods

### 105 2.1 Model description

106 LandscapeDNDC is a modular process-based ecosystem model for simulating the bio-  
107 geochemical change of C and N in croplands, forest and grassland systems at both site and  
108 regional scale. The modules combined are about plant growth, micro-meteorology, water  
109 cycling, physico-chemical-plant and microbial C and N cycling and exchange processes with  
110 atmosphere and hydrosphere of terrestrial ecosystems. LandscapeDNDC is a generality of the  
111 plant development and soil biogeochemistry of the agricultural DNDC and Forest-DNDC (Li,  
112 2000). There is a successful application of earlier model versions in a number of studies, e.g.  
113 water balance (Grote et al., 2009; Holst et al., 2010), plant growth (Cameron et al., 2013;  
114 Werner et al., 2012), NO<sub>3</sub> leaching (Kim et al., 2015; Thomas et al., 2016) and soil respiration  
115 and gas emission trace (Chirinda et al., 2011; Kraus et al., 2014; Molina-Herrera et al., 2015).  
116 For the initialization of LandscapeDNDC physical and chemical site-specific soil profile  
117 information is used (specified for different soil depths): Soil organic carbon (SOC) and nitrogen  
118 (SON) content, soil texture (clay, sand and silt content), of the plant growth and soil  
119 biogeochemistry, bulk density, pH value, saturated hydraulic conductivity, field capacity and  
120 wilting point. Daily or hourly climate data of air temperature (max, min and average), N  
121 deposition, precipitation, and atmospheric CO<sub>2</sub> concentration are used in LandscapeDNDC in  
122 combination with agricultural management practices e.g. crop planting and harvesting,  
123 fertilizing (synthetic and organic) or feed cutting and tilling are used to drive LandscapeDNDC  
124 simulations. Regarding fertilization management three types of mineral fertilizers, i.e. urea,  
125 compound fertilizers based on NH<sub>4</sub> and NO<sub>3</sub> as well as organic amendments, i.e. green  
126 manure, farmyard manure, slurry, straw, bean cake and compost are currently considered.



127 The growth of crops and grasses is similar to the DNDC approach using two major parameters  
128 that describe seasonal plant development (cumulative temperature degrees days) and  
129 maximum reachable biomass under optimum conditions (Li, 2000) while daily growth  
130 limitations due to water and nutrient availability are considered. Model parameters describing  
131 soil and vegetation characteristics are obtained from an external parameter library. In  
132 LandscapeDNDC, the parameterization of the main cultivated commodity crops in Europe  
133 occurs by default parameter sets representing an average plant type while process parameter  
134 values for micro-meteorology, water cycle and bio-geochemical processes were obtained from  
135 previous validation studies, e.g. (Klatt et al., 2015a; Molina-Herrera et al., 2016; Rahn et al.,  
136 2012) proving that the LandscapeDNDC model could be universally applicable for similar  
137 conditions.

138 For all simulations in the current study, site-specific crop parameterizations were derived in a  
139 preceding analysis of various site scale simulations and validations of yield characteristics  
140 across the region. An overview of the crops cultivated at the different study sites and detailed  
141 information on specific crop rotations used to simulate crop growth are provided in Table A2  
142 (supplementary material).

## 143 2.2 Case study description and input data

144 The region of Thessaly is located in Central Greece covering a total area of 14 000 Km<sup>2</sup>, where  
145 5000 Km<sup>2</sup> is lowland and approx. 2300 Km<sup>2</sup> and 6500 Km<sup>2</sup> are semi-mountainous and  
146 mountainous land respectively. The plain of Thessaly is considered to be among the largest  
147 agricultural land of the country (Kalivas et al., 2001) accounting for almost 410 000 ha, of which  
148 about 370 000 ha is arable land where almost 80% is covered by annual and 10% by perennial  
149 crops (ELSTAT, 2012). The crop/plant production of the region is around 14.2% (ELSTAT,  
150 2012) of the total production of the country (2<sup>nd</sup> in Greece).

151 Soil input data for the region was available from the European Project Nitro Europe IP (Sutton  
152 et al., 2013) based on the European Soil Database (ESDB v2.0, 2004) containing, soil type  
153 and soil profile description of bulk density, SOC content, texture (sand, silt clay), pH value,



154 stone fraction, saturated hydraulic conductivity, wilting point and water-holding capacity in  
155 various soil strata (Cameron et al., 2013). A regional soil dataset for the area of interest  
156 contained about 1500 spatial polygons out of which approximately 1000 covered the cultivated  
157 cropland that was finally simulated. The climate data for the regional simulations was derived  
158 at polygon level from gridded ERA5 climate data for Greece.

### 159 2.3 Agricultural Management and model input data processing

160 The total cultivated area and the respective yields for the years 2010 to 2016, used in the  
161 current analysis were obtained from the Hellenic Statistical Authority (ELSTAT). Moreover,  
162 data associated with the animal capital for the respective years was also provided (ELSTAT)  
163 in order to estimate the annual manure production distributed in the region however no data is  
164 available on whether and how much of the manure is used in croplands. For the water  
165 management, the percentage of irrigated and non-irrigated land (estimated to almost 50% for  
166 each case) was also given (ELSTAT) while indicative sets of irrigation management data were  
167 acquired through the River Basin Management Plans of the Special Secretariat for Water,  
168 Ministry of Environment and Energy (YPEKA, Portmann et al., 2010). The irrigation water  
169 volumes were estimated based on the crops needs and the minimum and maximum quantities  
170 necessary according to literature while using upscaling tools to get the regional values. The  
171 fertilization data sets were provided by Fertilizer Producers and Merchandiser Association  
172 (FPMA) for the recent years (2010-2016) and are equated to the annual consumed quantities  
173 on a national level, scaled down to a regional level based on crop pattern in the Region of  
174 Thessaly cultivated land.

175 In this study, the five main crops maize, wheat, clover, cotton and barley were considered,  
176 covering the majority of the cultivated arable land in the region (over 95%) while the remaining  
177 cropland was included acquiring the final corrected land/crop coverage. In Table 1 the resulting  
178 crop rotation scenarios (R1 - R5) are presented for the evaluation period 2012 - 2016. Note,  
179 each rotation sequence (R1 - R5) is shifted in time such that for each year, each crop appears  
180 exactly in one rotation. Based on the crop cover contribution in each simulated year the crop



181 rotation contribution factors were estimated and are summarized in Table 2. The management  
 182 practices were based on the general agricultural practices applied in the region and information  
 183 provided by farmers.

184

185 *Table 1. Summary of the crop rotation scenarios (R1- R5) for the region of Thessaly. The crop abbreviations corn,*  
 186 *wiwh, clover, cott and wbar refer to maize (food corn and silage maize), winter wheat, clover (legume feed crops*  
 187 *s.a. alfalfa or vetch), cotton and winter barley respectively.*

year	R1	R2	R3	R4	R5
2012	clover	cotton	wbar	corn	wiwh
2013	cotton	wbar	corn	wiwh	clover
2014	wbar	corn	wiwh	clover	cotton
2015	corn	wiwh	clover	cotton	wbar
2016	wiwh	clover	cotton	wbar	corn

188

189 *Table 2. Crop cultivation area contribution per year to the aggregation of the five rotations; data constant across*  
 190 *the region of Thessaly*

Crop Rotation Contribution [% / 100]					
Years	R1	R2	R3	R4	R5
2012	0.15	0.15	0.45	0.11	0.14
2013	0.13	0.29	0.09	0.10	0.39
2014	0.29	0.13	0.10	0.35	0.12
2015	0.15	0.11	0.43	0.16	0.16
2016	0.10	0.36	0.14	0.14	0.25

191

192

## 193 2.4 Uncertainty analysis

194 As stated in the IPCC 2006 guidelines and updated in 2019, the assessment of uncertainty is  
 195 considered a major and crucial/mandatory component when compiling regional or national  
 196 GHG emission inventories (Larocque et al., 2008). The difference in scale in which the model  
 197 is used results in divergent errors of the C and N dynamics prediction across different climate  
 198 zones and scales. Thus, uncertainty analysis is a crucial step towards a higher quality decision



199 making process. The sources of uncertainty can vary and are related to a) the initial conditions  
200 (starting values), b) the drivers (e.g. climate and crop management data), c) the conceptual  
201 model uncertainty and d) the parameter uncertainty of the various processes (Refsgaard et al.,  
202 2007; Wang and Chen, 2012).

203 Santarbarbara (2019) performed a Bayesian Model Calibration and Uncertainty Analysis using  
204 a Monte Carlo Markov Chain (MCMC) approach targeting uncertainties associated to the data  
205 (bulk density, SOC, pH, clay content) of the initial soil conditions, drivers (cropland  
206 management such as fertilization/manure rates & timing, harvest & seeding timing, tillage  
207 timing) and bio-geochemical process parameterizations.

208 In order to identify the most sensitive process parameters with a reduced number of model  
209 simulations, the Morris method (Morris, 1991) obtains a hierarchy of parameters influence on  
210 a given output (gaseous N fluxes) and evaluates whether a non-linearity exists or not. (Morris,  
211 1991) proposed that this order can be assessed through the statistical analysis of the changes  
212 in the model output, produced by the "one-step-at-a-time" changes in "n" number of proposed  
213 parameters. Incremental steps of each parameter range, lead to identifying which ones have  
214 substantial influences over the concerned results, without neglecting that some effects could  
215 cancel each other (Saltelli et al., 2000), leading to the identification of the 24 most sensitive  
216 process parameters (Houska et al., 2017; Myrriotis et al., 2018b).

217

#### 218 2.4.1 Metropolis – Hastings algorithm

219 The Markov Chain Monte Carlo (MCMC) Metropolis–Hastings algorithm results in numerous  
220 parameter sets that approximate the posterior joint parameter distribution by performing a  
221 random walk through the space of joint parameter values. This probability evaluation of the  
222 data obtained from each step leads to the update of the initial uniform parameter distributions.  
223 Bayes' formula relating conditional probabilities may become a powerful and practical  
224 computational tool when combined with Markov chain processes and Monte Carlo methods,  
225 so-called Markov Chain Monte Carlo (MCMC). A Markov chain is a special type of discrete



226 stochastic processes wherein the probability of an event depends only on the event that  
227 immediately precedes it. Integrating parameters ( $\theta$ ) and observation data ( $D$ ) into Bayes' rule  
228 results in the formula:  
229

$$P(\theta|D) = \frac{P(D|\theta) * P(\theta)}{P(D)} \quad 2.1$$

230 where  $P(D|\theta)$ , the probability of the data, is used to obtain the probability of these parameters  
231 updated by the data:  $P(\theta|D)$  where the evidence is computed as:  
232

$$P(D) = \int \text{likelihood} \cdot \text{prior} \cdot d\theta \quad 2.2$$

233 where  $P(D)$  can be numerically approximated with the aforementioned MCMC method (Robert  
234 and Casella, 2011).

235 The method uses prior knowledge concerning the sources of the model uncertainty to obtain  
236 a narrowed posterior distribution for each one of the sources. By propagating the parameter  
237 distributions through the model, the overall uncertainty in the model results can be quantified.  
238 In the current analysis, 500 joint parameter sets were sampled from the posterior distributions  
239 in combination with input data perturbations as reported by Santabarbara (2019) and were  
240 deployed in simulations (propagation through the model) for the regional inventory leading to  
241 500 inventory simulations. A statistical analysis was, afterwards, applied to estimate the  
242 updated regional and temporal result distributions.

243

## 244 2.5 Statistical methods and data aggregation

### 245 2.5.1 Regional result aggregation

246 One full regional inventory simulation consists of 10 individual inventory simulations: Five (5)  
247 different crop rotations for irrigated and rain feed conditions were simulated in parallel (see  
248 section 2.3). The results of the crop rotations were aggregated according to the crop shares



249 per year (see Table 2) accounting for all effects of the different crops cultivated in the region  
250 for irrigated and rain feed conditions. The final inventory simulation results were obtained by  
251 considering irrigated versus rain feed water management. The final inventory contains  
252 simulation results aggregated to area weighted yearly means across the total simulation  
253 domain accounting for the cropland area of each polygon.

254

### 255 2.5.2 Uncertainty quantification and statistical analysis

256 A regional aggregation was performed for all 500 uncertainty simulations. All the uncertainty  
257 results were finally reported via statistical measures evaluating the 500 regional uncertainty  
258 simulation runs reporting mean values, standard deviation, medians and the 25 and 75  
259 interquartile ranges (IQR, Q25 to Q75).

260

## 261 3 Results Analysis and Evaluation

262 The simulation time span was from 2009 to 2016, while the years 2009 – 2011 were used as  
263 spin-up to get all soil C and N pools into equilibrium after the initialization. Therefore, reported  
264 simulation results are limited to years 2012 - 2016. The assessment of the regional C and N  
265 balances (CB and NB) were obtained - as a consequence of the uncertainty quantification -  
266 resulting in distributions and therefore reported by statistical measures such as mean/median  
267 or interquartile ranges of the uncertainty ensemble.

268

### 269 3.1 Regional yield simulations and validation

270 The evaluation of the model performance in estimating the NB and CB components was  
271 analyzed based on the comparison of the simulated yield values with the observed yield data  
272 provided by the Hellenic Statistical Authority (ELSTAT), averaged for the total simulated  
273 period.

274



275 3.1.1 Crop yields and feed production

276 For model validation, datasets of crop yields from Hellenic Statistical Authority (ELSTAT) were  
277 used. Table 3 summarizes the aggregated regional crop yields for all the simulated years and  
278 the respective mean, median and standard deviation values resulted from the statistical  
279 analysis of the simulation results together with the observed yield and feed production provided  
280 by the Hellenic Statistical Authority (ELSTAT). Simulated yields consist for cotton of the cotton  
281 bolls, clover feed is the total cutting and harvested above ground biomass, for wheat and barley  
282 is the grain yield and for maize is accounted grain ear and the stems. Based on the  
283 observations, maize appears to be the dominant crop with an average yield of 12 tons ha<sup>-1</sup>,  
284 followed by clover product of 8.4 tons ha<sup>-1</sup>. The rest of the three crop yields appear to be in the  
285 same order of magnitude from 3.3 up to 3.4 tons ha<sup>-1</sup>.

286

287 *Table 3. Simulated and observed yields and feed production [tons dry matter ha<sup>-1</sup>] in the region of Thessaly. All*  
288 *results are based on statistical aggregation across all polygons, rotations, years and finally across all 500 UA*  
289 *inventory simulations. The observed values of dry matter (DM) are provided by the Hellenic Statistical Authority.*

Simulated crop yield and feed distributions [tons dry matter ha <sup>-1</sup> ]				Observed [tons dry matter ha <sup>-1</sup> ]
Crops	Median	Mean	standard deviation	Mean
Cotton	3.5	3.3	0.8	3.3
Clover	9.8	9.6	0.6	8.4
Wheat	3.9	3.6	0.9	3.4
Barley	4.7	4.5	1.0	3.3
Maize <sup>1)</sup>	10.2	9.9	1.4	12.0

290 <sup>1)</sup> Observation data for maize did not distinguish between food corn and silage maize.

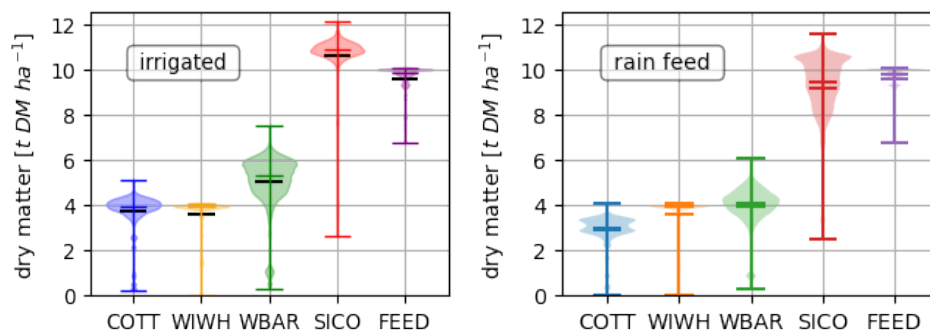
291

292 Additionally, the simulated average yield of cotton was estimated to 3.3 ± 0.8 tons DM ha<sup>-1</sup>,  
293 wheat to 3.6 ± 0.9 tons DM ha<sup>-1</sup>, barley 4.5 ± 1 tons DM ha<sup>-1</sup>, maize 9.9 ± 1.4 tons DM ha<sup>-1</sup>. As  
294 for the feed, the clover was estimated to 9.6 ± 0.6 tons DM ha<sup>-1</sup>. The average nitrogen use  
295 efficiency (NUE) across time and space is 63.29%.

296



297 Figure 1 presents the uncertainties of the simulated crop yield across the whole evaluation  
298 time span 2012 -2016 both in irrigated and rain feed conditions. As shown, corn shows a much  
299 more narrow distribution with a higher median for the irrigated scenario compared to the rain  
300 feed while shows the same extreme value variations. To the contrary, winter barley has a wider  
301 distribution and slightly higher median for the irrigated scenario and, also, a wider extreme  
302 value variation. As for cotton, the distribution appears to be bimodal for the rain feed scenario  
303 in which the median is also lower than the one in the irrigated case. In addition, the extreme  
304 value variation is wider in the latter case. Finally, for the example of winter wheat irrigated and  
305 rain feed scenarios reach the same results.  
306



307  
308 *Figure 1. Simulated crop yield uncertainties across the evaluation time span 2012 - 2016 for irrigated and rain feed*  
309 *conditions. Horizontal lines indicate median, mean, maximum and minimum values of the distributions.*

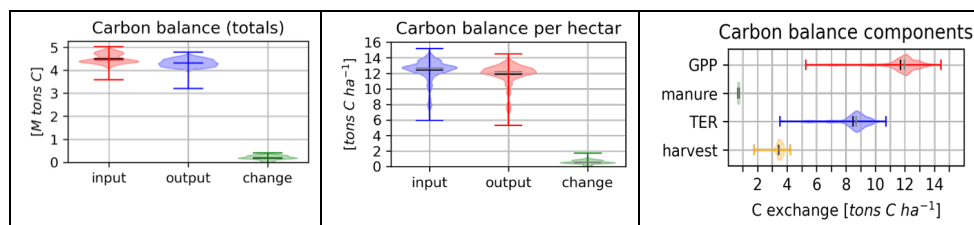
310  
311 **3.2 Regional Carbon and Nitrogen Balance**

312 **3.2.1 Carbon Balance (CB)**

313 For the CB, Figure 2 presents average C input fluxes into the soil of  $12.4 \pm 1.4$  tons C ha<sup>-1</sup> yr<sup>-1</sup>  
314 <sup>1</sup> (with inter quartile ranges (IQR) from Q25 to Q75 of 12.1 to 13.2 tons C ha<sup>-1</sup> yr<sup>-1</sup>) and output  
315 fluxes of  $11.9 \pm 1.3$  tons C ha<sup>-1</sup> yr<sup>-1</sup> with IQR from 11.6 to 12.7 tons C ha<sup>-1</sup> yr<sup>-1</sup>. The resulting  
316 carbon sequestration was estimated to  $0.5 \pm 0.3$  tons C ha<sup>-1</sup> yr<sup>-1</sup> with IQR from 0.4 to 0.7 tons  
317 C ha<sup>-1</sup> yr<sup>-1</sup> (data summarized in Table 4).



318



319 Figure 2. Carbon balance for cropland cultivation for the region of Thessaly: a) Total carbon balance of cropland  
 320 soils in mio. tons C, b) averaged Carbon Balance in tons C ha<sup>-1</sup> and c) averaged fluxes across the region and the  
 321 years 2012-2016. (Positive change equals soil C sequestration).

322

323 The input fluxes consist of annual gross primary productivity (GPP) of  $11.7 \pm 1.4$  tons C ha<sup>-1</sup>  
 324 yr<sup>-1</sup> with IQR from 11.4 to 12.4 tons C ha<sup>-1</sup> yr<sup>-1</sup> and carbon applied to soils in manure estimated  
 325 by  $0.7 \pm 0.001$  tons C ha<sup>-1</sup> yr<sup>-1</sup> (see Table 4). This compares on the other hand to respirative  
 326 carbon fluxes from the soil to the atmosphere (TER) of  $8.5 \pm 1.1$  tons C ha<sup>-1</sup> yr<sup>-1</sup> with IQR from  
 327 8.2 to 9.1 tons C ha<sup>-1</sup> yr<sup>-1</sup> and carbon fluxes via exported crop yields and feed (including all  
 328 straws and removed crop residues) of  $3.4 \pm 0.3$  tons C ha<sup>-1</sup> yr<sup>-1</sup> with IQR from 3.4 to 3.6 tons  
 329 C ha<sup>-1</sup> yr<sup>-1</sup>. The aggregation of the carbon fluxes to the regional level of approx. 360 000 ha of  
 330 cropland results in  $4.25 \pm 0.20$  M tons C yr<sup>-1</sup> by GPP,  $0.25 \pm 0.01$  M tons C yr<sup>-1</sup> carbon influx  
 331 via organic fertilizers compared to  $3.08 \pm 2.97$  M t C yr<sup>-1</sup> TER and  $1.24 \pm 0.05$  M t C yr<sup>-1</sup> carbon  
 332 exports via crop yields and feed production leading to a net carbon sequestration of  $0.5 \pm 0.3$   
 333 M tons C ha<sup>-1</sup> yr<sup>-1</sup> with IQR from 0.4 to 0.7 M tons C ha<sup>-1</sup> yr<sup>-1</sup> (M tons C as Million tons carbon).

334

335 Table 4. **Carbon Balance** (per hectare) Assessment and Uncertainty Analysis of the of cropland cultivation at the  
 336 region of Thessaly, Greece. <sup>1)</sup> mean; <sup>2)</sup> standard deviation; <sup>3)</sup> median; Interquartile ranges: <sup>4)</sup> Q25: 25 quartile, <sup>5)</sup>  
 337 Q75: 75 quartile are applied across the 500 values for the quantities in this table; <sup>6)</sup> C-Inputs as the sum of the  
 338 absolute values of all the input fluxes of the 500 simulations; <sup>7)</sup> C-Outputs as the sum of the absolute values of all  
 339 the output fluxes of the 500 simulations; <sup>8)</sup> SOC-changes as the difference between the input and output fluxes of  
 340 each of the 500 simulations.

	Mean <sup>1)</sup>	Std <sup>2)</sup>	Median <sup>3)</sup>	Q25 <sup>4)</sup>	Q75 <sup>5)</sup>
	[tons C ha <sup>-1</sup> yr <sup>-1</sup> ]				
C-Inputs <sup>6)</sup>	12.4	1.4	12.7	12.1	13.2

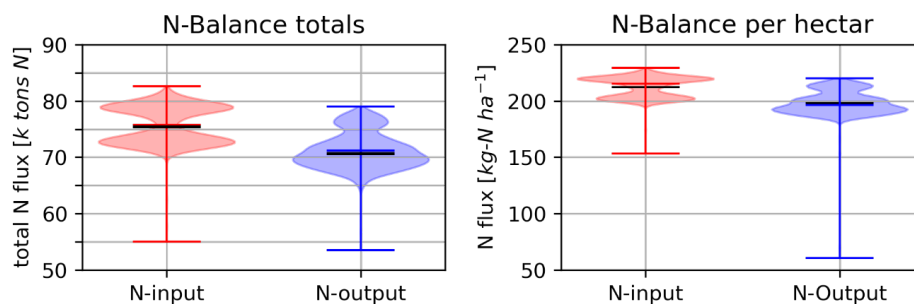


C-Outputs <sup>7)</sup>	11.9	1.3	12.2	11.6	12.7
SOC-changes <sup>8)</sup>	0.5	0.3	0.5	0.4	0.7
Input fluxes					
GPP	11.7	1.4	12.0	11.4	12.4
C in manure	0.7	0.0	0.7	0.7	0.7
Output fluxes					
TER	8.5	1.1	8.7	8.2	9.1
Biomass export	3.4	0.3	3.5	3.4	3.6

341

### 342 3.2.2 Nitrogen balance (NB)

343 In



344

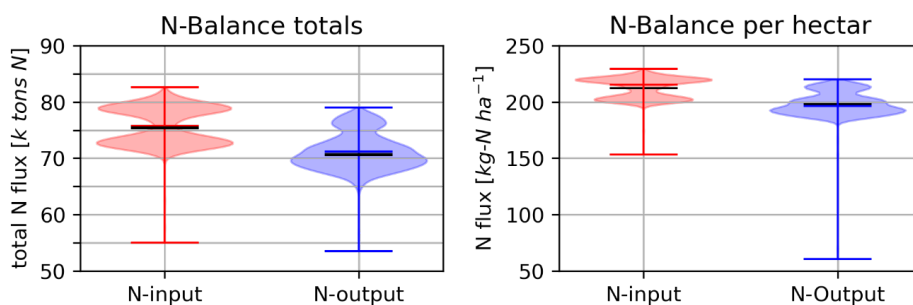
345 Figure 3 the assessment of the distribution of the NB with the in- and out-fluxes is presented.

346 The averaged nitrogen influx (represented by the uncertainty ensemble mean) per hectare was

347 estimated to  $212.3 \pm 9.1 \text{ kg N ha}^{-1} \text{ yr}^{-1}$  with IQR from 203.3 to 220.0  $\text{kg N ha}^{-1} \text{ yr}^{-1}$  while nitrogen

348 out-fluxes were estimated in average to  $198.3 \pm 11.2 \text{ kg N ha}^{-1} \text{ yr}^{-1}$  with IQR from 191.4 to

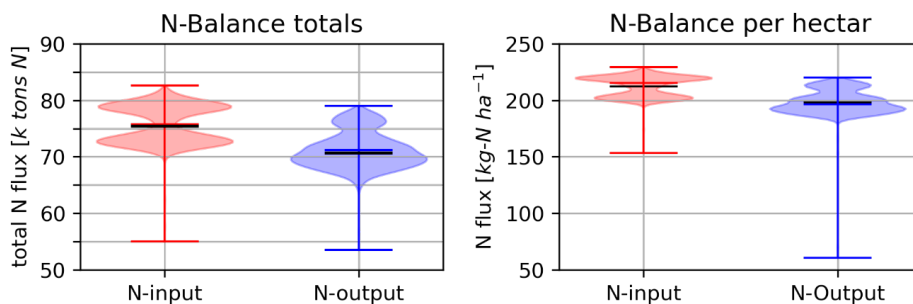
349  $204.0 \text{ kg N ha}^{-1} \text{ yr}^{-1}$  (



350

351 Figure 3) leading to a net N accumulation in the soil of  $14.0 \pm 2.1 \text{ kg N ha}^{-1} \text{ yr}^{-1}$  with IQR from  
 352 11.9 to  $16.0 \text{ kg N ha}^{-1} \text{ yr}^{-1}$ .

353



354

355 Figure 3. Nitrogen balance for cropland cultivation for the region of Thessaly; a) Total NB in k-tons N and b)  
 356 averaged NB in  $\text{kg N ha}^{-1}$ ; Data averaged for the years 2012-2016. Horizontal lines indicate mean (red), median  
 357 and minimum and maximum of the distribution.

358

359 Table 5. Nitrogen Balance (per hectare). Summary of the Assessment and Uncertainty Analysis of the **NB Fluxes**  
 360 (per hectare) of cropland cultivation of the region of Thessaly, Greece. <sup>1)</sup> N-Inputs as the sum of the absolute values  
 361 of all input fluxes of the 500 simulations; <sup>2)</sup> N-Outputs as the sum of the absolute values of all the output fluxes of  
 362 the 500 simulations; <sup>3)</sup> N-stock-changes as the difference between the input and output fluxes of each of the 500  
 363 simulations; <sup>4)</sup> Gaseous emissions are the sum of  $\text{N}_2\text{O}$ , NO,  $\text{N}_2$  and  $\text{NH}_3$  fluxes; <sup>5)</sup> Aquatic flux is nitrate leaching  
 364 ( $\text{NO}_3^-$ ).

	Mean	Std	Median	Q25	Q75
	[ $\text{kg N ha}^{-1} \text{ yr}^{-1}$ ]				
N-Inputs <sup>1)</sup>	212.3	9.1	215.2	203.3	220.0
N-Outputs <sup>2)</sup>	198.3	11.2	196.4	191.4	204.0
N-stock-changes <sup>3)</sup>	13.8	2.1	13.7	14.5	12.5

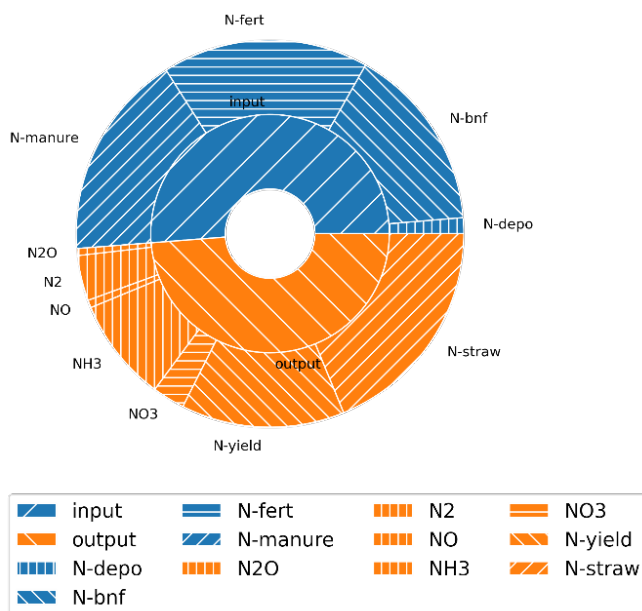


Input fluxes					
N deposition	6.3	0.8	6.8	6.0	6.8
Bio. N fixation	45.6	4.3	45.7	43.7	47.7
N in min. fertilizer	80.2	4.8	81.3	76.6	82.7
N in organic fertilizer	80.2	3.6	80.9	77.5	82.7
Output fluxes					
Gaseous emissions <sup>4)</sup>	55.4	8.8	55.1	48.9	61.6
N <sub>2</sub> O	2.6	0.8	2.5	2.1	3.1
NO	3.2	1.5	2.9	2.0	4.1
N <sub>2</sub>	15.5	7.0	14.6	9.9	20.7
NH <sub>3</sub>	34.0	6.7	31.8	29.3	36.9
Aquatic fluxes <sup>5)</sup>					
NO <sub>3</sub> leaching	14.1	4.5	13.6	11.0	17.0

365

366 The N influx was composed by the input of synthetic fertilizer of  $80.2 \pm 4.8$  kg N ha<sup>-1</sup> yr<sup>-1</sup> (IQR  
 367 76.6 to 82.7) and organic fertilizer of  $80.2 \pm 3.6$  kg N ha<sup>-1</sup> yr<sup>-1</sup> (IQR from 77.5 to 82.7), followed  
 368 by the biological nitrogen fixation (BNF) via legumes estimated as  $45.6 \pm 4.3$  kg N ha<sup>-1</sup> yr<sup>-1</sup> (IQR  
 369 from 43.7 to 47.7) and nitrogen deposition of  $6.3 \pm 0.8$  kg N ha<sup>-1</sup> yr<sup>-1</sup> (IQR from 6.0 to 6.8). Thus,  
 370 almost 75% of the nitrogen input influx is related to the fertilization (mineral and organic) whilst  
 371 the minor part that corresponds to nitrogen fixation and deposition approximates to 25%.

372 The N outflux consist of gaseous N fluxes of  $55.4 \pm 8.8$  kg N ha<sup>-1</sup> yr<sup>-1</sup> (IQR from 48.9 to 61.6),  
 373 aquatic N fluxes (only nitrate leaching into surface waters was considered) of  $14.1 \pm 4.5$  kg N  
 374 ha<sup>-1</sup> yr<sup>-1</sup> (IQR from 11.0 to 17.0), N fluxes by removed N in yields, straw and feed of  $128.8 \pm$   
 375  $8.5$  kg N ha<sup>-1</sup> yr<sup>-1</sup> (IQR of 125.2 to 131.7) (see Figure 4 and Table 5). Based on the  
 376 aforementioned results all gaseous and aquatic N-fluxes correspond to about 28% and 7% of  
 377 the N output flux respectively, while the far largest N output flux was N removed in yields, straw  
 378 and feed representing almost 65% of the N outflux (Figure 4).



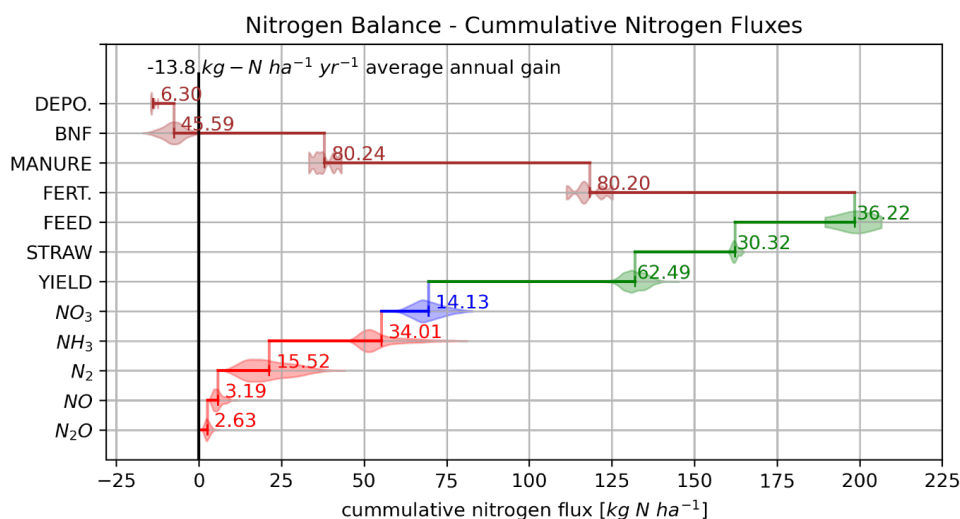
379

380 *Figure 4. Averaged annual nitrogen balance (inner ring of the pie diagram) and their decomposition into the various*  
 381 *components of the N fluxes (outer ring of the pie diagram); (all data summarized in Table 5).*

382

383 The simulated gaseous fluxes were composed of N<sub>2</sub>O emissions estimated to 2.6 ± 0.8 kg  
 384 N<sub>2</sub>O-N ha<sup>-1</sup> yr<sup>-1</sup> (IQR from 2.1 to 3.1), NO emissions of 3.2 ± 1.5 kg NO-N ha<sup>-1</sup> yr<sup>-1</sup> (IQR from  
 385 2.0 to 4.1), N<sub>2</sub> emissions 15.5 ± 7.0 kg N<sub>2</sub>-N ha<sup>-1</sup> yr<sup>-1</sup> (IQR range from 9.9 to 20.7) and NH<sub>3</sub>  
 386 emissions of 34.0 ± 6.7 kg NH<sub>3</sub>-N ha<sup>-1</sup> yr<sup>-1</sup> (IQR from 29.3 to 36.9). Ammonia volatilization  
 387 represents the largest share (61.48%) of gaseous N losses, with highest densities in the  
 388 emission distribution between approx. 25 and 35 kg N ha<sup>-1</sup>, followed by di-nitrogen losses  
 389 (28.03%) of gaseous N losses, with a much wider emission variability in the distribution,  
 390 followed by NO<sub>3</sub> (5.79%) and N<sub>2</sub>O (4.7%). Figure 5 shows the overall NB in a waterfall diagram  
 391 adding up cumulative all in- and out-fluxes illustrating the uncertainty distribution of each flux  
 392 contributions. The waterfall diagram illustrates the overall outcome of the NB, a N accumulation  
 393 into the soil as the difference between all out-fluxes minus all in-fluxes.

394



395

396 *Figure 5. Waterfall representation of the result distributions of the different Nitrogen in- and outfluxes of the cropland*  
 397 *cultivation in Thessaly. Vertical lines in the distributions indicate mean values of the corresponding N-flux. Red*  
 398 *colors indicate gaseous outfluxes, blue aquatic fluxes, green biomass yield and feed production outfluxes and brown*  
 399 *color indicates N influxes such as synth. N-fertilizer, N-Manure, biological N fixation (BNF) and N deposition. The*  
 400 *Resulting N sink of the Nitrogen Balance (based on distribution means) is -13.8 kg N ha<sup>-1</sup> yr<sup>-1</sup>. (Negative value*  
 401 *indicates flux into the soil).*

402

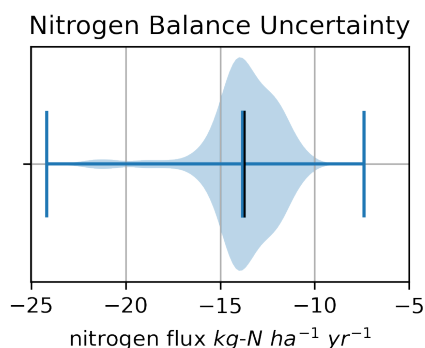
403 Nitrate leaching mean estimates were  $14.1 \pm 4.5$  kg NO<sub>3</sub>-N ha<sup>-1</sup> yr<sup>-1</sup> (IQR from 11.0 to 17.0)  
 404 with a bell-shaped distribution.

405 Total yield and biomass (straw and feed) N export fluxes were  $62.4 \pm 4.4$  kg N ha<sup>-1</sup> yr<sup>-1</sup> with  
 406 uncertainty ranges from 59.9 to 65.1 consisting of yield N exports (grains and cotton balls) of  
 407  $30.3 \pm 1.7$  kg N ha<sup>-1</sup> yr<sup>-1</sup> (IQR from 29.6 to 30.9) and for straw and feed N exports of  $36.1 \pm 6.0$   
 408 kg N ha<sup>-1</sup> yr<sup>-1</sup> (IQR from 34.9 to 37.6). The result distributions for yield N are well bell shaped,  
 409 for feed biomass N very moderate bell shaped and well distributed within the bounds and for  
 410 straw N very sharp within a comparable small interval.

411 Figure 5 illustrates the cumulative nitrogen fluxes composing the NB as a waterfall diagram  
 412 considering the mean of each component. The NB results in a net N sink of  $13.8$  kg N ha<sup>-1</sup> yr<sup>-1</sup>  
 413 <sup>1</sup> (see result distribution in Figure 6) for the region corresponding to an annual carbon  
 414 sequestration of approx. 0.5 tons C ha<sup>-1</sup> yr<sup>-1</sup> as depicted in Figure 2 b) (see also the annual  
 415 dynamics of the topsoil (30 cm) soil organic carbon and nitrogen distributions in Figure 8).



416

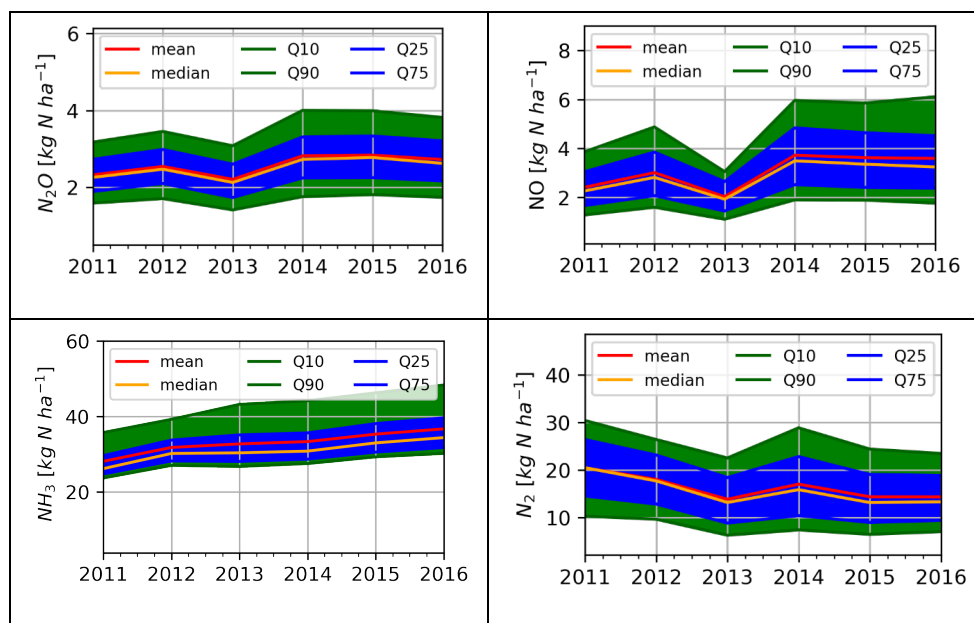


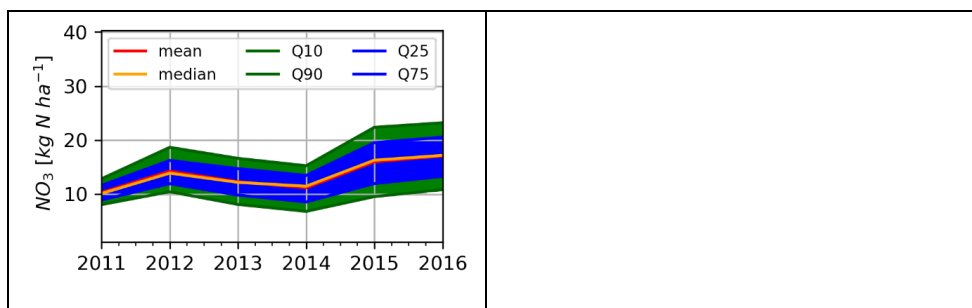
417

418 *Figure 6. Distribution of the overall Nitrogen Balance of the cropland cultivation in Thessaly: Statistical analysis*  
419 *across all 500 individual NB results of the inventory simulations (mean 13.8 kg N ha<sup>-1</sup> yr<sup>-1</sup>, median 13.7 kg N ha<sup>-1</sup>*  
420 *yr<sup>-1</sup>) corresponding to the Carbon balance in Figure 2.*

421

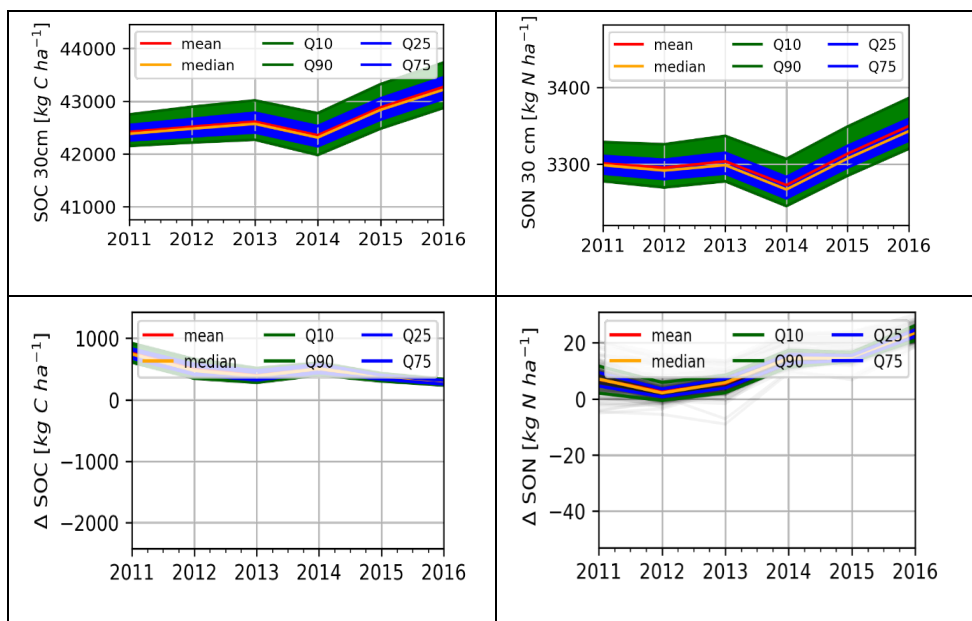
422 Figure 7 and Figure 8 show the dynamics of the annual distribution of the gaseous and aquatic  
423 outfluxes as well as the dynamics of the annual distributions of the top soil (30 cm) soil organic  
424 carbon and nitrogen pools for the evaluation period 2011 – 2016.





425 Figure 7. Annual dynamics of the uncertainty distributions of the gaseous (subfigure a) to d)) and aquatic (subfigure  
426 e)) N outfluxes 2011 – 2016. Uncertainty bandwidth (blue band) defined as the range between the q25 and the q75  
427 quartile, green band (Q10. to Q90 interval) indicating the variance of the fluxes neglecting the outliers of the  
428 distribution.

429



430 Figure 8. Annual dynamics of the uncertainty distributions of the soil carbon (subfigure a)) and soil organic nitrogen  
431 (subfigure b)) and the corresponding dynamics of the uncertainty distributions of the annual change rates of the  
432 total soil carbon and nitrogen pools (subfigures c) and d)) respectively.

#### 433 4 Discussion.

434 Simulating the N and C budgets is helpful for the understanding/explanation of the pattern how  
435 nutrients are being supplied from the soil to crop as well as the pathways of the excess  
436 gaseous and aquatic excess nitrogen fluxes. In this way, improvements on the agricultural  
437 practices e.g. N fertilization strategy could be accomplished to sustain agricultural output and



438 minimize environmental harm. In this study, an assessment of the full C and N balance of a  
439 regional cropland agroecosystem is reported for the first time using inventory simulations with  
440 a process-based ecosystem model in combination with the quantification of the associated  
441 modelling uncertainty. Up to present, process-based modelling studies mainly focus on single  
442 site applications e.g. Daycent: (del Grosso et al., 2005; Gurung et al., 2020), APSIM: (Vogeler  
443 et al., 2013), CERES-EGC: (Dambreville et al., 2008; Gabrielle et al., 2006; Heinen, 2006;  
444 Hénault et al., 2005), CERES-Wheat: (Mavromatis, 2016), DNDC: (Li, 2000),  
445 LandscapeDNDC: (Haas et al., 2013; Klatt et al., 2015a; Molina-Herrera et al., 2016; Zhang et  
446 al., 2015). Fewer studies deploy models on the regional to national (del Grosso et al., 2005;  
447 Kim et al., 2015; Klatt et al., 2015a) or continental to global scale (del Grosso et al., 2009;  
448 Franke et al., 2020; Jägermeyr et al., 2021; Smerald et al., 2022; Thompson et al., 2019). All  
449 of these studies focus in general on one specific or a few components of the carbon or nitrogen  
450 cycle such as e.g. soil carbon stocks or N<sub>2</sub>O emissions.

451 There are very few cases where an attempt for regional estimation of the NB has been made.  
452 Schroeck et al., (2019) reported an assessment of the NB for a large alpine watershed in the  
453 Austrian Alps characterized by arable production in the low-lying areas and grassland in the  
454 mountains. In addition, Lee et al., (2020) tried to estimate nitrogen balances in Switzerland  
455 alternating the cropping systems or management practices. There were, also, cases where  
456 the regional NB was estimated with the use of nitrogen balance equations (He et al., 2018).

457 In order to achieve a more concrete and complete analysis of the CB and NB that could be  
458 used for future policy development, an uncertainty analysis is considered as  
459 necessary/mandatory. The IPCC guidelines demand for UNFCCC reporting the uncertainty  
460 quantification of any reported inventory study (IPCC Updated guidelines 2019). Recent  
461 publications have reported the deployment of different methods to assess and quantify the  
462 various sources of uncertainty in ecosystem modelling. (Klatt et al., 2015b) published a study  
463 on the impact of parameter uncertainty on N<sub>2</sub>O emissions and NO<sub>3</sub> leaching on the regional  
464 scale. (Houska et al., 2017) deployed the GLUE method (Generalized Likelihood Uncertainty  
465 Estimation) for the LandscapeDNDC model on a grassland site, others studies such as



466 (Lehuger et al., 2009a; Li et al., 2015; Myrgiotis et al., 2018a) used the Bayesian Model  
467 Calibration and Uncertainty Assessment approach, which has been used in the current study  
468 as well.

469

#### 470 4.1 Yield and feed Production

471 A number of studies including crop yields estimates under different environmental conditions  
472 and crop management options have been published. Molina-Herrera et al., (2016) reported  
473 validation results deploying LandscapeDNDC on cropland and grassland sites across Europe.

474 The study reported good agreement in reproducing observed above ground biomass and yield  
475 estimates leading to a high trustworthiness of model results. Similar model performance for  
476 the cultivation of commodity crops was reported by (Kasper et al., 2019; Klatt et al., 2015a;  
477 Molina-Herrera et al., 2017; R. J. Petersen et al., 2021)

478 Voloudakis et al., (2015) simulated cotton production in seven different areas of Greece  
479 applying the AquaCrop model for future climate scenarios. The model was calibrated and the  
480 results were validated with data sets acquired for years 2006 and 2005/2007 respectively from  
481 a site experiment conducted in the area of Karditsa, Thessaly. The observed and simulated  
482 results presented in the study were well matched and in line with the results presented in our  
483 study with averaged yields of 3.65 tons ha<sup>-1</sup> (mean 3.3 tons ha<sup>-1</sup> and median 3.5 tons ha<sup>-1</sup>).

484 Lyra and Loukas, (2021) used REPIC model to estimate the crop growth/yield production of  
485 several crops in the Basin of Almyros, Thessaly. The simulated results were approximately 11  
486 tons ha<sup>-1</sup> clover, 3.3/3.5 tons ha<sup>-1</sup> cereals/wheat, 3.8 tons ha<sup>-1</sup> cotton and 9 tons ha<sup>-1</sup> maize,  
487 being well compared to the results of the current research shown in Table 3.

488 The application of AquaCrop in the cotton cultivation of the research of Tsakmakis et al.,  
489 (2019), proved the accurate estimation of the cotton yield when using the default set of  
490 parameters in both cases of growing degree days (GDD) and calendar days (CD) modes for a  
491 site in Northern Greece. For the year of 2015 the harvested seed cotton yield was 3.974 tons  
492 ha<sup>-1</sup> ± 0.45 and 3.35 tons ha<sup>-1</sup> ± 0.397 in 2016 with a slight overestimation of 0.018 tons ha<sup>-1</sup>



493 and 0.026 tons ha<sup>-1</sup> while in 2016 there was a marginal underestimation by 0.06 tons ha<sup>-1</sup> and  
494 0.046 tons ha<sup>-1</sup> for the respective aforementioned cases. The model did not perform well when  
495 the parameter sets were altered based on other studies (García-Vila et al., 2009).

496 There are few cases in literature concerning yield simulations on a European level. Based on  
497 the yield datasets of FAO and EUROSTAT Ciais et al., (2010a) estimated mean crop yields  
498 for the period 1990–1999 at the scale of EU-25 as 6.1 (FAO) and 5.3 (EUROSTAT) tons DM  
499 ha<sup>-1</sup> yr<sup>-1</sup>, respectively, which corresponds well to results of our study. Haas et al., (2022)  
500 estimated with a model ensemble mean for crop yields for EU-27 of 4.41 ± 1.85 tons DM ha<sup>-1</sup>  
501 yr<sup>-1</sup> for the period 1990–1999. Lugato et al., (2018) estimated cropland yield projections of  
502 4.34 tons DM ha<sup>-1</sup> yr<sup>-1</sup> (mean), ranging from 3.69 to 4.90 tons DM ha<sup>-1</sup> yr<sup>-1</sup> with the DayCent  
503 model for EU-27, comparable to the 6.18 tons DM ha<sup>-1</sup> yr<sup>-1</sup> average simulated crop yields of  
504 this study. The simulated yields in the current study vary from 3.3 to 9.9 tons DM ha<sup>-1</sup> yr<sup>-1</sup> for  
505 the cases of cotton and maize respectively.

506 Higher yield estimates for the region of Thessaly in this study are certainly due to the inclusion  
507 of the legume feed crops in the rotations. This argument is supported by a recent meta-analysis  
508 by (Lu, 2020) that concluded that on average yield increases of 5.0 to 25% can be expected  
509 for various conditions if residues are completely returned to the field as compared to no-residue  
510 return systems. Similar results were reported by Fuchs et al., (2020) and Barneze et al., (2020).

511

## 512 4.2 Carbon and Nitrogen Balance:

### 513 4.2.1 SOC stocks

514 Haas et al., (2022) reported results of a European inventory simulation of soil carbon stocks  
515 and N<sub>2</sub>O emissions using a model ensemble. The study deployed in a baseline simulation  
516 across EU-27 a similar residues management as compared to our study resulting in very stable  
517 carbon stock dynamics over a long period (1950-2100). In this study, the estimated carbon  
518 sequestration of 0.5 (UA mean and median) ± 0.3 tons C ha<sup>-1</sup> yr<sup>-1</sup> is mainly caused by the  
519 inclusion of legume feed crops within the crop rotation leading to increased litter production



520 and C input into the soil (Barneze et al., 2020; Fuchs et al., 2020; K. Petersen et al., 2021).  
521 Haas et al., (2022) reported a management scenario with 100% of crop litter remaining on the  
522 field leading to averaged C-sequestration rates of over 1 ton C ha<sup>-1</sup> yr<sup>-1</sup> across EU-27. As the  
523 residues management in this study is between the baseline and buried scenario of Haas et al.,  
524 (2022), our results compare well to results reported in this study.

525 Other studies such as (Lugato et al., 2014) reported C sequestration rates for the conversion  
526 of cropland into grassland ranging between 0.4 and 0.8 tons C ha<sup>-1</sup> yr<sup>-1</sup>. Lugato et al., (2014)  
527 reported averaged SOC change rates for a cereal straw incorporation scenario for EU-27 of  
528 0.1 tons C ha<sup>-1</sup> yr<sup>-1</sup> (estimates from 2000 to 2020).

529 The Mediterranean agroecosystems show a winter/summer rainfall and soil cover variation,  
530 spatial diversity, and the longest continuous settlement and dense cultivation by man (Yaalon,  
531 1997). Based on the Greek National Map of SOC (2020) by Triantakonstantis and Detsikas,  
532 (2021), SOC values for the region of Thessaly vary from 22.95 to 86.97 tons ha<sup>-1</sup> with the lower  
533 values in the main plain of the region and higher values in the croplands closer to the  
534 mountainous areas. Comparing these maps with SOC map of the 30cm topsoil of our story,  
535 we clearly see similar patterns, which relate to the similarity of SOC data used to initialize the  
536 region in LandscapeDNDC.

537

#### 538 4.2.2 N<sub>2</sub>O emissions

539 This study reported estimates of N<sub>2</sub>O emissions of 2.6 ± 0.8 kg N<sub>2</sub>O-N ha<sup>-1</sup> yr<sup>-1</sup> (IQR from 2.1  
540 to 3.1) for a mixed crop / legume feed crop rotation. The LandscapeDNDC validation study of  
541 Molina-Herrera et al., (2016) reported for the Italian site Borgo Cioffi (Mediterranean climate,  
542 Ranucci et al., (2011) annual N<sub>2</sub>O emissions of 2.49 kg N<sub>2</sub>O-N ha<sup>-1</sup> yr<sup>-1</sup> while two sites in  
543 southern France showed annual N<sub>2</sub>O emissions from 0.52 to 3.34 kg N<sub>2</sub>O-N ha<sup>-1</sup> yr<sup>-1</sup>. N<sub>2</sub>O  
544 emission estimates of our study were higher than results reported by Haas et al., (2022) using  
545 a multi model ensemble estimating average soil N<sub>2</sub>O emissions from European (EU-27)



546 cropping systems for the period 1980–1999 of  $1.46 \pm 1.30 \text{ kg N}_2\text{O-N ha}^{-1} \text{ yr}^{-1}$  under  
547 conventional (*Baseline*) management and comparable average N input.

548 Leip et al., (2011) applied the DNDC–Europe model across EU-25 reporting averaged  $\text{N}_2\text{O}$   
549 emissions of  $1.8 \text{ kg N}_2\text{O-N ha}^{-1} \text{ yr}^{-1}$ , while on basis of UNFCCC reporting and a fuzzy logic  
550 model Ciais et al., (2010b) estimated average  $\text{N}_2\text{O}$  emissions from EU-27 croplands at  $1.46 \pm$   
551  $0.22 \text{ kg N}_2\text{O-N ha}^{-1} \text{ yr}^{-1}$ .

552 Klatt et al., (2015a) reported for an inventory (Saxony, Germany) mean  $\text{N}_2\text{O}$  emission of  $1.43$   
553  $\pm 1.25 \text{ kg N}_2\text{O-N ha}^{-1} \text{ yr}^{-1}$  using a very similar uncertainty quantification approach.

554 As discussed by Haas et al., (2022) and Janz et al., (2022), increased  $\text{N}_2\text{O}$  emissions can be  
555 seen after the addition of crop residues and may be attributed to a stimulation of denitrification  
556 activity by the added substrate and the creation of anaerobic microsites by increased soil  
557 respiration.

558 Arable land cultivation in Thessaly does not experience strong winter frost and severe soil  
559 freezing such that  $\text{N}_2\text{O}$  freeze-thaw emissions as reported by Wagner-Riddle et al., (2017) or  
560 del Grosso et al., (2022) do not play any role in the N budget.

561 The  $\text{N}_2\text{O}$  estimations related to livestock presented in the study of Sidiropoulos and  
562 Tsilingiridis, (2009) varied in a range of 0.74 to 4.33 kt  $\text{N}_2\text{O}$ , with an average of 2.84 kt  $\text{N}_2\text{O}$   
563 depended on the average values of emission factors used (for the year 2005). The estimates  
564 were based on the emission factors of IPCC guidelines and the number of animal heads were  
565 derived from the data sets acquired from the Hellenic Statistical Authorities as in the current  
566 study.

567 Cayuela et al., (2017) conducted a meta-analysis of the direct  $\text{N}_2\text{O}$  emissions for a number of  
568 cropping systems for the Mediterranean climate where the emission factors (EFs) were altered  
569 under different fertilization and irrigation conditions. Higher fertilization rates led to higher EFs  
570 (0.82% less than the 1% of IPCC). Additionally, irrigated and intensively cultivated crops had  
571 higher EFs than rainfed (up to 0.91% dependent on the irrigation method). The relatively high  
572 EF of maize in this study could be possibly attributed to the irrigation without the application of  
573 water-saving methods and the on average higher N application rates (Cayuela et al., 2017).



574

#### 575 4.2.3 Nitrate leaching

576 This study reported average NO<sub>3</sub> leaching fluxes (only nitrate leaching into surface waters) of  
577 14.1 ± 4.5 kg NO<sub>3</sub>-N ha<sup>-1</sup> yr<sup>-1</sup>. Molina-Herrera et al., (2016) reported for the LandscapeDNDC  
578 validation study cropland nitrate leaching fluxes of approx. 7 to 88 kg NO<sub>3</sub>-N ha<sup>-1</sup> yr<sup>-1</sup>. In  
579 addition, in the research of Molina-Herrera et al., (2017) the described NO<sub>3</sub> leaching results  
580 varied from 13 to 8 kg NO<sub>3</sub>-N ha<sup>-1</sup> yr<sup>-1</sup> from 2009 to 2012 showing higher values in regards to  
581 the precipitation and fertigation. The most comparable site Borgo Cioffi resulted in a  
582 comparable annual NO<sub>3</sub> leaching flux of 18.62 kg NO<sub>3</sub>-N ha<sup>-1</sup> yr<sup>-1</sup>. de Vries et al., (2011)  
583 estimated the NO<sub>3</sub> leaching with the use of four different models with varying values from 5 to  
584 40 kg NO<sub>3</sub>-N ha<sup>-1</sup> yr<sup>-1</sup> for the area of our study. These high values could be explained by the  
585 fact that it corresponds both to groundwater and runoff. Klatt et al., (2015b) reported in an  
586 uncertainty assessment for a regional inventory (Saxony, Germany) leaching rates of 29.32 ±  
587 9.97 kg NO<sub>3</sub>-N ha<sup>-1</sup> yr<sup>-1</sup> for a wheat-barley-rapeseed rotation simulated by the LandscapeDNDC  
588 model. The agricultural system and management regime is comparable; higher NO<sub>3</sub> leaching  
589 rates were most likely due to higher N fertilization rates (up to 150 kg N) compared with higher  
590 annual precipitation in the region leading to more intense percolation and therefore to stronger  
591 leaching of available NO<sub>3</sub> while in our study the fertilization regime was more lean (up to  
592 average of 80 kg N input) such that soil nutrient competition was higher and available nitrate  
593 was more likely to be immobilized by plant uptake.

594

#### 595 4.2.4 NO emissions

596 In the current study, the model estimated NO emissions were in average 3.2 ± 1.5 kg NO-N  
597 ha<sup>-1</sup> yr<sup>-1</sup>. Butterbach-Bahl et al., (2009) performed the very first European inventory of soil NO  
598 emissions using a modified version of DNDC reporting low NO emission rates mostly below 2  
599 kg NO-N ha<sup>-1</sup> yr<sup>-1</sup>. Molina-Herrera et al., (2017) recently reported a full NO emission inventory  
600 for the State of Saxony Germany compiling annual NO emissions from agricultural soils



601 ranging from 0.19 to 6.7 kg NO-N ha<sup>-1</sup> yr<sup>-1</sup> simulated by LandscapeDNDC. The study reported  
602 the model performance on simulating soil NO emissions on more than 20 different sites. The  
603 study of Schroeck et al., (2019) reported for a regional inventory of arable soils in Austria  
604 simulated by LandscapeDNDC annual NO emissions of 1.0–1.5 kg NO-N ha<sup>-1</sup> (for the year  
605 2000), while empirical approaches such as Stehfest and Bouwman, (2006) estimated emission  
606 of similar magnitude. Zhang et al., (2015) reported in a model inter-comparison and validation  
607 study of NO and N<sub>2</sub>O fluxes including three ecosystem models, consistent simulation results  
608 for the LandscapeDNDC model with NO emission strengths of cropland soils were between 1  
609 and 3 kg NO-N ha<sup>-1</sup> yr<sup>-1</sup> across the sites.

610

#### 611 4.2.5 NH<sub>3</sub> emissions

612 Schroeck et al., (2019) stated that validation studies of NH<sub>3</sub> volatilization for any  
613 biogeochemical model were very rarely reported in literature, mainly due to the complexity and  
614 a lack of flux observations at spatial and temporal high resolution.

615 In our study the assessment of soil NH<sub>3</sub> emissions of 34.0 ± 6.7 kg NH<sub>3</sub>-N ha<sup>-1</sup> yr<sup>-1</sup>. High NH<sub>3</sub>  
616 volatilization and emission rates can be explained by the predominating neutral to basal soils  
617 conditions (pH values of 7 and above) in the study region favouring the Henry NH<sub>4</sub>/NH<sub>3</sub>  
618 equilibrium towards higher NH<sub>3</sub> gases enabling ammonia to diffuse out of the soil into the free  
619 atmosphere.

620 The IPCC emission factor (EF) method for NH<sub>3</sub> volatilization reports estimates of 20% of N  
621 input into the soil to be volatilized as NH<sub>3</sub>. For our study, IPCC methodology for NH<sub>3</sub> would  
622 lead to 16 kg NH<sub>3</sub>-N ha<sup>-1</sup> yr<sup>-1</sup>, which is approximately half the emission strength of the  
623 simulated result. This is due to the neglect of soil properties in the IPCC EF approach which  
624 in contrast is reflected in the modelling approach.

625 Sidiropoulos and Tsilingiridis, (2009) estimated a national livestock originated NH<sub>3</sub> value of  
626 about 40 kt NH<sub>3</sub> yr<sup>-1</sup> of the total 73 kt NH<sub>3</sub> yr<sup>-1</sup> for Greece and the year 2005, which corresponds



627 to approx. 22 kg ha<sup>-1</sup> yr<sup>-1</sup> for the region of Thessaly (the arable land in the region accounts for  
628 20% of the national).

629 Ramanantenasoa et al., (2018) compared two methods CADASTRE\_NH3 and the one of  
630 CITEPA in France on a regional and national level in order to estimate the NH<sub>3</sub> emissions and  
631 emission factors. CADASTRE\_NH3 is a combination of spatial and temporal databases of  
632 meteorological, soil and N fertilizing data with the process-based Volt'Air model, on small  
633 agricultural regions scale. CITEPA is the organism responsible for the national inventories  
634 where the applied methodology is using a number of statistical data excluding the synthetic  
635 and organic fertilizer properties as well as the cultural practices. Their first model gave lower  
636 results than the second by 29%, being, though, higher than the reported in literature range of  
637 uncertainties. This difference was mainly explained as a difference in the observed applied N  
638 and ammoniacal-N (TAN) giving lower estimates of CADASTRE\_NH3 emissions by 63% for  
639 the applications of the organic manure.

640 There is a number of national NH<sub>3</sub> inventories which could be considered detailed and well-  
641 studied like the ones in Denmark, Netherlands, Europe, UK and US. In Denmark, (Geels et al.,  
642 2012) used the DAMOS model to estimate the Danish NH<sub>3</sub> emissions (crop, grass and manure  
643 manipulation) where the values ranged in the 5 regions under study from a very small quantity  
644 to 17.4 kg NH<sub>3</sub>-N ha<sup>-1</sup> yr<sup>-1</sup>. In the case of the Netherlands (Velthof et al., 2012), a method was  
645 applied based on the estimation of total N excretion and the Total Ammoniacal N (TAN)  
646 percentage in the later. The total national estimated NH<sub>3</sub> emission was 88.8 Gg NH<sub>3</sub>-N for the  
647 year 2009, of which the majority (87%) was related to the housing and manure estimation. de  
648 Vries et al., (2011) used four N budget models of varying complexity for the estimation of the  
649 most common N fluxes in EU27. In the case of NH<sub>3</sub> emissions all the models give very  
650 comparable results, which based on their spatial distribution varied from 0-10 kg NH<sub>3</sub>-N ha<sup>-1</sup>  
651 yr<sup>-1</sup> for our region under study. The result might differ from our estimated simulation since it is  
652 based on a set of emission factors.

653 As discussed by Sutton et al., (2013) the majority of the NH<sub>3</sub> emissions come as a result of the  
654 agricultural production and are considerably impacted by climate influence. In the case of NH<sub>3</sub>



655 volatilization, it could almost double every 5°C temperature given certain complex  
656 thermodynamics dissociation and solubility, whilst soil NH<sub>3</sub> emission is influenced by the  
657 available water quantity allowing the NH<sub>x</sub> dissolution and use by microbial organisms, which is  
658 afterwards leading to decomposition.

659

#### 660 4.2.6 Full N balance

661 At present, the studies of Schroeck et al., (2019) and Lee et al., (2020) are the only to be found  
662 by Web of Science under the search key words “nitrogen AND balance AND process AND  
663 based AND modelling” reporting a compilation of the nitrogen balance for a site or region  
664 applying a process-based ecosystem model even though IPPC is explicitly demanding such  
665 attempts.

666 Leip et al., (2011) reported the first nitrogen balance for Europe following mixed approach  
667 combining the CAPRI (Common Agricultural Policy Regionalised Impact) model (a global  
668 economic model for agriculture) with different approaches estimating various nitrogen fluxes  
669 in arable land cultivation. The approach e.g. lacks to explicit quantification of the gaseous N  
670 fluxes. The study of Schroeck et al., (2019) overcame this hurdle and applied the process-  
671 based ecosystem model LandscapeDNDC to estimate the full regional nitrogen budgets of  
672 different ecosystems (cropland, grassland and pastures) and climatic zones of a water shed in  
673 Austria. That is a considerable contribution to the attempt for estimating all the N fluxes  
674 possible since only a few countries could offer measurement networks, which could supply  
675 inventory estimates for independent validation Ogle and Paustian, (2005).

676 The N<sub>2</sub>O estimate in Schroeck et al., (2019) and the current study is of a comparable level. In  
677 the later research, the estimated value was 2.6 kg N ha<sup>-1</sup> yr<sup>-1</sup> while Schroeck et al., (2019)  
678 reports 1.51 kg N ha<sup>-1</sup> yr<sup>-1</sup> lower about 40%. The NO fluxes differ by far since we reported a  
679 mean value of 3.2 kg NO-N ha<sup>-1</sup> yr<sup>-1</sup> while Schroeck et al., (2019) reports 0.08 kg NO-N ha<sup>-1</sup>  
680 yr<sup>-1</sup>. This is related to some recent model advances, which have been made during this study,  
681 which elevated the NO production in LandscapeDNDC (Molina-Herrera et al., 2017). Ammonia



682 volatilization differs, also, substantially between the two studies. Our study reports 34 kg NH<sub>3</sub>-  
683 N ha<sup>-1</sup> yr<sup>-1</sup> and Schroeck et al., (2019) moderate emissions of 0.23 kg NH<sub>3</sub>-N ha<sup>-1</sup> yr<sup>-1</sup>. The  
684 stronger NH<sub>3</sub> volatilization in our study is mostly driven by the high pH-values of the soils in  
685 the region of Thessaly (pH values from 6.5 to 8.2 with a considerable spatial variation, Greek  
686 Soil Map, 2015) and the comparable high manure inputs of arable system in our study, while  
687 in the research of Schroeck et al., (2019) the manure was preferably applied to the grassland  
688 systems and mineral fertilizers to the arable land. Concerning the NO<sub>3</sub>, Schroeck reported 45.3  
689 kg NO<sub>3</sub>-N ha<sup>-1</sup> yr<sup>-1</sup> which 3 times higher compared to this study (14.1 kg N ha<sup>-1</sup> yr<sup>-1</sup>)  
690 considering the N- input of approximately 140 kg and 212.3 kg N ha<sup>-1</sup> yr<sup>-1</sup> respectively.

691 The N balance modelling study of Lee et al., (2020) is estimating for Switzerland a national  
692 cropland N balance using an upscaling method based on process-based site simulations with  
693 the DayCent model differentiating the management of the considered cropping systems e.g.  
694 fertilizer rates, tillage or land cover change. The study reported for conventional cultivations  
695 (averaged across 20 years) yield related N outputs accounting for about 60%, NO<sub>3</sub>- leaching  
696 36.1% and gaseous N emissions 4.1% of the total N outputs. Although the yield related N  
697 output is in accordance with our result of 64.95% there seems to be a discrepancy in the  
698 gaseous and aquatic N fluxes contribution, 27.94% and 7.11% respectively, which could  
699 possibly occur due to the differences in the soil and climatic conditions, or the arable crops  
700 included in the respective researches.

701 Velthof et al., (2009) used the MITTERA-EUROPE model/method, based on the concoction of  
702 GAINS and CAPRI models, to estimate N fluxes of European soils on NUTS2 scale with the  
703 use of European datasets and literature coefficients, where the fertilizer application and  
704 management was similar to our methodology. The average N Input-Output balance was  
705 calculated as 117 kg N ha<sup>-1</sup> yr<sup>-1</sup> composed by manure of 49 kg N ha<sup>-1</sup> yr<sup>-1</sup>, synthetic fertilizer of  
706 58 kg N ha<sup>-1</sup> yr<sup>-1</sup> (in the current study for both cases 80.2 kg N ha<sup>-1</sup> yr<sup>-1</sup>), biological nitrogen  
707 fixation of 2 kg N ha<sup>-1</sup> yr<sup>-1</sup> (our research 45.6 kg N ha<sup>-1</sup> yr<sup>-1</sup>) and N deposition of 7 kg N ha<sup>-1</sup>  
708 (current study 6.3 kg N ha<sup>-1</sup> yr<sup>-1</sup>). In contrast to our study the reported output fluxes for NH<sub>3</sub> of  
709 8 kg NH<sub>3</sub>-N ha<sup>-1</sup> yr<sup>-1</sup>, N<sub>2</sub>O of 2 kg N<sub>2</sub>O-N ha<sup>-1</sup> yr<sup>-1</sup>, NO<sub>x</sub> of 2 kg NO<sub>x</sub>-N ha<sup>-1</sup> yr<sup>-1</sup>, N<sub>2</sub> of 51 kg N<sub>2</sub>-N



710  $\text{ha}^{-1} \text{yr}^{-1}$  and  $\text{NO}_3$  leaching of  $7 \text{ kg NO}_3\text{-N ha}^{-1} \text{yr}^{-1}$  while the differences with the results presented  
711 in our study are  $\text{NH}_3$  of  $34.0 \text{ kg NH}_3\text{-N ha}^{-1} \text{yr}^{-1}$ ,  $\text{N}_2\text{O}$  of  $2.6 \text{ kg N}_2\text{O -N ha}^{-1} \text{yr}^{-1}$ ,  $\text{NO}_x$  of  $3.2 \text{ kg}$   
712  $\text{NO}_x \text{-N ha}^{-1} \text{yr}^{-1}$ ,  $\text{N}_2$  of  $15.5 \text{ kg N ha}^{-1} \text{yr}^{-1}$  and  $\text{NO}_3$  leaching of  $14.1 \text{ kg NO}_3\text{-N ha}^{-1} \text{yr}^{-1}$ .  
713 Additionally, the yield output is estimated as  $48 \text{ kg N ha}^{-1} \text{yr}^{-1}$ . The difference with the results  
714 presented in our study, could be related to the different input data used, based on regional  
715 statistics and the use of a biogeochemical model and not on literature factors as in the later  
716 study.

717 He et al., (2018) assessed the soil N balance for a time span between 1984 to 2014 based on  
718 the N budget equations ( $\text{N input} - \text{N output}$ ) using multiple coefficients from literature in order  
719 to estimate the nitrogen input and output fluxes of six grouped regions in China. The used  
720 datasets were acquired from national Authorities and include cropping land and yields,  
721 synthetic fertilizers, animal heads, soil types etc. The N synthetic fertilizer input is in average  
722  $182.4 \text{ kg N ha}^{-1}$  and the organic fertilizer of  $97.3 \text{ kg N ha}^{-1}$ , N fixation is estimated as  $16.8 \text{ kg}$   
723  $\text{N ha}^{-1}$  and the atmospheric deposition as  $22 \text{ kg N ha}^{-1}$ . Almost half of the total averaged N  
724 output losses, 48.9%, was attributed to crop uptake while the respective gaseous losses were  
725  $\text{N}_2$  19.9%, volatilized  $\text{NH}_3$  17.3%,  $\text{N}_2\text{O}$  1.2% and  $\text{NO}$  0.7%. As for the  $\text{NO}_3$  leaching share was  
726 5.8% of the total output N fluxes. The previous results are comparable to the results of the  
727 current study mainly in the aquatic fluxes, which account for approx. 7%, as described in Figure  
728 4. The difference that appears in the N uptakes could be a result of the fact that in our study it  
729 includes the yield, straws and feed.

730 Myrriotis et al., (2019) reported a  $\text{N}_2\text{O}$  emission factor (EF) estimate for arable land of 0.59%  
731 and associated uncertainty bands of  $\pm 0.36\%$  which is half of the  $\text{N}_2\text{O}$  EF of our study of approx.  
732 1.2% (data not shown). The reported  $\text{NO}_3$  leaching factor (LF) mean for their region was 14%  
733 ( $\pm 7\%$ ). Myrriotis reported an averaged NUF of 37 % ( $\pm 7\%$ ) which is almost half of the NUF  
734 of 67.3% we reported in the current study.

735 As reported in OECD (OECD Nutrient Balance, 2020) the averaged nitrogen input rate for  
736 Greece is estimated at about  $290 \text{ kg N ha}^{-1}$  for the years 2010-2015. Based on the regional  
737 land share (~20% of the national arable land) the nitrogen balance of the area under study



738 becomes  $11.6 \text{ kg N ha}^{-1} \text{ yr}^{-1}$ . As presented in Table 5 the simulated mean nitrogen balance  
739 results in an in-flux of  $13.8 \text{ kg N ha}^{-1} \text{ yr}^{-1}$  (IQR 11.9 to 16.0) which is well in line with the  
740 aforementioned OECD value.

741

#### 742 4.3 Uncertainty Analysis and Quantification

743 The MCMC algorithm was used by Santabarbara (2019) to estimate the joint parameter  
744 distribution of the fundamental bio-geochemical process parameters in LandscapeDNDC  
745 when simulation soil C and N fluxes. Propagating these joint parameter distributions through  
746 the model (by sampling 500 joint parameter distributions and performing inventory simulations  
747 with each parameter set with the model) for estimating the regional C and N fluxes was leading  
748 to distributions for any model result on the regional scale. Statistical analysis calculating mean,  
749 median as well as the interquartile range (Q25 to Q75) determines best estimates and the  
750 uncertainty range of any model output on the regional scale, demonstrating the superiority of  
751 the method for assessing any ecosystem response by modelling instead of reporting single  
752 results. This is a novel approach, that to our knowledge has not been reported before in  
753 literature for the carbon and nitrogen balance and neither been applied to regional simulations  
754 by any process-based model.

755 In this study, the estimated UA mean and median of the carbon sequestration of  $0.5 \pm 0.3 \text{ tons}$   
756  $\text{C ha}^{-1} \text{ yr}^{-1}$  is associated with an uncertainty range from 0.4 to 0.7  $\text{tons C ha}^{-1} \text{ yr}^{-1}$  which  
757 compares well to the spatial uncertainty of C-sequestration in the study of Haas et al., (2022).

758 The approach used in this study enabled to assess the carbon and nitrogen balance of the  
759 cropland ecosystems including an assessment of the prediction uncertainty.

760 van Oijen et al., (2005) used the Bayesian calibration method to acquire the parameter  
761 posterior probability distribution to sample from, for simulation of the model results. Lehuger et  
762 al., (2009b) used the Bayesian calibration method for the enhancement of the CERES-EGC  
763 model parameterization (reduction of the apriori parameter distribution) as well as  
764 quantification of the uncertainty of the simulated  $\text{N}_2\text{O}$  emissions in different sites. The



765 estimated fluxes of the different sites resulted in a range between 0.088 to 3.672 kg N<sub>2</sub>O-N ha<sup>-1</sup>  
766 yr<sup>-1</sup> with values for the q05 quantile of 0.066 to 0.115 kg N<sub>2</sub>O-N ha<sup>-1</sup> yr<sup>-1</sup> and for the Q95  
767 quantile from 1.676 to 5.874 kg N<sub>2</sub>O-N ha<sup>-1</sup> yr<sup>-1</sup> with an averaged value of 1.04 kg N<sub>2</sub>O-N ha<sup>-1</sup>  
768 yr<sup>-1</sup> which is lower than the result of the current study but still in the same order of magnitude.  
769 Klatt et al., (2015b) quantified a parameter-induced uncertainty analysis on the regional scale  
770 applying the LandscapeDNDC model for simulating N<sub>2</sub>O emission and NO<sub>3</sub> leaching  
771 inventories similar to our study. The region was represented by 4000 polygons of arable land  
772 (state of Saxony, Germany) for crop rotations of barley, wheat and rapeseed. The investigated  
773 model parameter related uncertainties give a high confidence for the parameter use in our  
774 research. The results of Klatt et al., (2015b) display a likelihood range of 50% (the IQR range  
775 between Q25 and Q75) for N<sub>2</sub>O emissions from 0.46 to 2.05 kg N<sub>2</sub>O-N ha<sup>-1</sup> yr<sup>-1</sup> which is in  
776 good comparison to our results of 2.1 to 3.1 kg N<sub>2</sub>O-N ha<sup>-1</sup> yr<sup>-1</sup>. The average direct N<sub>2</sub>O  
777 emissions are 1.43 kg N<sub>2</sub>O-N ha<sup>-1</sup> yr<sup>-1</sup> comparable to the result of our study (mean: 2.6 and  
778 median: 2.5 kg N<sub>2</sub>O-N ha<sup>-1</sup> yr<sup>-1</sup> across approx. 1000 polygons). As for leached NO<sub>3</sub>, Klatt et  
779 al., (2015b) reported leaching rates of mean value: 29 kg NO<sub>3</sub>-N ha<sup>-1</sup> yr<sup>-1</sup>, (IQR from 24.5 to  
780 36.0), which is higher compared to the results of our study: Mean: 14.1 kg NO<sub>3</sub>-N ha<sup>-1</sup> yr<sup>-1</sup>,  
781 median: 13.6 kg NO<sub>3</sub>-N ha<sup>-1</sup> yr<sup>-1</sup> (IQR from 11 to 17).  
782 Butterbach-Bahl et al., (2022) reported the influence of management uncertainties for  
783 compiling national inventories of CH<sub>4</sub> and N<sub>2</sub>O emission from various rice cultivation systems  
784 in Vietnam. The study applied a sampling technique varying model input data within a given  
785 range and analyzing the influence on the assessed CH<sub>4</sub> and N<sub>2</sub>O emission strengths. As the  
786 underlying cropland systems were fundamentally different, the assessed uncertainty ranges  
787 were comparable and the study is supporting our approach to focus on reporting uncertainty  
788 ranges rather than single values.  
789 The current study postulates a novel approach to report regional scale C and N fluxes from  
790 process-based models to become the standard reporting method fulfilling the long-time  
791 demanded reporting requirements of the IPCC (IPCC Guidelines and IPCC 2019 updates on  
792 Guidelines). Additionally, instead of focusing only on topics limited to soil carbon stocks



793 dynamics or greenhouse gas emissions, we propose the report of the full C and N balance  
794 including all components of the various fluxes e.g. gaseous and/or aquatic being available by  
795 the individual process-based models. This constitutes an effective method to assess the  
796 environmental impact of the crop production on a national scale, therefore optimize the farming  
797 practices, and suggest possible solution for sustainable agriculture development.

798  
799

## 800 5 Conclusion

801

802 In this research, we presented for the first time a regional inventory of the full carbon and  
803 nitrogen balance including all sub-components of these fluxes simulated by a process-based  
804 model. Additionally, the study has fulfilled the demand to report always the associated  
805 uncertainties for any modelling results being published in literature. This supports the  
806 trustworthiness of the reported results. The LandscapeDNDC model is applied in the region of  
807 Thessaly after using the MCMC Bayesian calibration method against soil, daily climatic and  
808 crop management regional datasets. The main scope/goal was the assessment of the total C  
809 and N balance that enhance the efforts towards the understanding of the cropland system and  
810 the respective interactions within the C and N balances.

811 Observed GHG emission datasets are scarce if not unavailable. Thus, the modelled yield  
812 results were evaluated/validated against the observed values of crop yields provided by the  
813 Hellenic Statistical Authority and showed a good fit for almost all simulated crops except for  
814 the case of maize where there was a slight underestimation.

815 In addition, a full uncertainty analysis is presented based on the Metropolis-Hastings algorithm  
816 where a parameter subset and input data preturbation was sampled and simulated in 500  
817 iterations resulting in a final probability density function (PDF) for each one of the N and C  
818 balance fluxes building a full uncertainty analysis of the modelled results. This helps to build  
819 trustworthiness in modelling assessments and estimates.



820 All of the above constitute the novelty of the conducted research that could be further  
821 elaborated by a number of proposed mitigation measures, which could help in the abatement  
822 of the GHG emissions and N fluxes from crop/agricultural land.

823

## 824 6 Acknowledgements

825 The author Odysseas Sifounakis received a Ph.D. research scholarship from Alexandros S.  
826 Onassis Public Benefit Foundation, Greece, part of which is the research presented in the  
827 current publication.

828

## 829 7 Code/Data availability

830 The LandscapeDNDC model source code is available via Butterbach-Bahl, Klaus; Grote,  
831 Rüdiger; Haas, Edwin; et al. (2021): LandscapeDNDC (v1.30.4). Karlsruhe Institute of  
832 Technology (KIT). DOI: 10.35097/438

833 All publication results (tables and data for figures) will be made available in the supplementary  
834 material associated with this paper.

835

836

## 837 8 Author contributions

838 Mr. Odysseas Sifounakis has conceived and designed the analysis and collected the data. He,  
839 also, performed the analysis and wrote the paper.

840 Dr. Edwin Haas conducted research and wrote the paper.

841 Prof. Dr. Klaus Butterbach-Bahl substantially contributed to research planning, manuscript  
842 writing and editing and, also, provided funding opportunities.

843 Prof. Dr. Maria P. Papadopoulou substantially contributed to research planning, manuscript  
844 writing and editing, and provided funding opportunities.

845



846 9 Competing interests

847 All authors have reviewed and accepted the submitted version and declare no conflicts of  
848 interest related to this publication.

849

850 10 References

851 2019 Refinement to the 2006 IPCC Guidelines for National Greenhouse Gas Inventories —  
852 IPCC [WWW Document], n.d. URL [https://www.ipcc.ch/report/2019-refinement-to-the-](https://www.ipcc.ch/report/2019-refinement-to-the-2006-ipcc-guidelines-for-national-greenhouse-gas-inventories/)  
853 [2006-ipcc-guidelines-for-national-greenhouse-gas-inventories/](https://www.ipcc.ch/report/2019-refinement-to-the-2006-ipcc-guidelines-for-national-greenhouse-gas-inventories/) (accessed 1.12.19).

854 Barneze, A.S., Whitaker, J., McNamara, N.P., Ostle, N.J., 2020. Legumes increase grassland  
855 productivity with no effect on nitrous oxide emissions. *Plant Soil* 446, 163–177.  
856 <https://doi.org/10.1007/s11104-019-04338-w>

857 Bell, M.J., Jones, E., Smith, J., Smith, P., Yeluripati, J., Augustin, J., Juszczak, R., Olejnik, J.,  
858 Sommer, M., 2012. Simulation of soil nitrogen, nitrous oxide emissions and mitigation  
859 scenarios at 3 European cropland sites using the ECOSSE model. *Nutr Cycl Agroecosyst*  
860 92, 161–181. <https://doi.org/10.1007/s10705-011-9479-4>

861 Butterbach-Bahl, K., Baggs, E.M., Dannenmann, M., Kiese, R., Zechmeister-Boltenstern, S.,  
862 2013. Nitrous oxide emissions from soils: How well do we understand the processes and  
863 their controls? *Philosophical Transactions of the Royal Society B: Biological Sciences*.  
864 <https://doi.org/10.1098/rstb.2013.0122>

865 Butterbach-Bahl, K., Kahl, M., Mykhayliv, L., Werner, C., Kiese, R., Li, C., 2009. A European-  
866 wide inventory of soil NO emissions using the biogeochemical models DNDC/Forest-  
867 DNDC. *Atmos Environ* 43, 1392–1402.  
868 <https://doi.org/10.1016/J.ATMOSENV.2008.02.008>

869 Butterbach-Bahl, K., Kraus, D., Kiese, R., Mai, V.T., Nguyen, T., Sander, B.O., Wassmann, R.,  
870 Werner, C., 2022. Activity data on crop management define uncertainty of CH<sub>4</sub> and N<sub>2</sub>  
871 O emission estimates from rice: A case study of Vietnam. *Journal of Plant Nutrition and*  
872 *Soil Science*. <https://doi.org/10.1002/jpln.202200382>



- 873 Camargo, J.A., Alonso, Á., 2006. Ecological and toxicological effects of inorganic nitrogen  
874 pollution in aquatic ecosystems: A global assessment. *Environ Int.*  
875 <https://doi.org/10.1016/j.envint.2006.05.002>
- 876 Cameron, D.R., van Oijen, M., Werner, C., Butterbach-Bahl, K., Grote, R., Haas, E., Heuvelink,  
877 G.B.M., Kiese, R., Kros, J., Kuhnert, M., Leip, A., Reinds, G.J., Reuter, H.I., Schelhaas,  
878 M.J., de Vries, W., Yeluripati, J., 2013. Environmental change impacts on the C- and N-  
879 cycle of European forests: A model comparison study. *Biogeosciences* 10, 1751–1773.  
880 <https://doi.org/10.5194/bg-10-1751-2013>
- 881 Cayuela, M.L., Aguilera, E., Sanz-Cobena, A., Adams, D.C., Abalos, D., Barton, L., Ryals, R.,  
882 Silver, W.L., Alfaro, M.A., Pappa, V.A., Smith, P., Garnier, J., Billen, G., Bouwman, L.,  
883 Bondeau, A., Lassaletta, L., 2017. Direct nitrous oxide emissions in Mediterranean  
884 climate cropping systems: Emission factors based on a meta-analysis of available  
885 measurement data. *Agric Ecosyst Environ* 238, 25–35.  
886 <https://doi.org/10.1016/j.agee.2016.10.006>
- 887 Chirinda, N., Kracher, D., Lægdsmand, M., Porter, J.R., Olesen, J.E., Petersen, B.M., Doltra,  
888 J., Kiese, R., Butterbach-Bahl, K., 2011. Simulating soil N<sub>2</sub>O emissions and heterotrophic  
889 CO<sub>2</sub> respiration in arable systems using FASSET and MoBiLE-DNDC. *Plant Soil* 343,  
890 139–160. <https://doi.org/10.1007/s11104-010-0596-7>
- 891 Ciais, P., Wattenbach, M., Vuichard, N., Smith, P., Piao, S.L., Don, A., Luysaert, S.,  
892 Janssens, I.A., Bondeau, A., Dechow, R., Leip, A., Smith, P.C., Beer, C., van der werf,  
893 G.R., Gervois, S., van oost, K., Tomelleri, E., Freibauer, A., Schulze, E.D., 2010a. The  
894 European carbon balance. Part 2: Croplands. *Glob Chang Biol* 16, 1409–1428.  
895 <https://doi.org/10.1111/j.1365-2486.2009.02055.x>
- 896 Ciais, P., Wattenbach, M., Vuichard, N., Smith, P., Piao, S.L., Don, A., Luysaert, S.,  
897 Janssens, I.A., Bondeau, A., Dechow, R., Leip, A., Smith, P.C., Beer, C., van der werf,  
898 G.R., Gervois, S., van oost, K., Tomelleri, E., Freibauer, A., Schulze, E.D., 2010b. The  
899 European carbon balance. Part 2: Croplands. *Glob Chang Biol* 16, 1409–1428.  
900 <https://doi.org/10.1111/j.1365-2486.2009.02055.x>



- 901 Dambreville, C., Morvan, T., Germon, J.C., 2008. N<sub>2</sub>O emission in maize-crops fertilized with  
902 pig slurry, matured pig manure or ammonium nitrate in Brittany. *Agric Ecosyst Environ*  
903 123, 201–210. <https://doi.org/10.1016/j.agee.2007.06.001>
- 904 Davidson, E.A., Kanter, D., 2014. Inventories and scenarios of nitrous oxide emissions.  
905 *Environmental Research Letters* 9. <https://doi.org/10.1088/1748-9326/9/10/105012>
- 906 de Vries, W., Leip, A., Reinds, G.J., Kros, J., Lesschen, J.P., Bouwman, A.F., 2011.  
907 Comparison of land nitrogen budgets for European agriculture by various modeling  
908 approaches. *Environmental Pollution* 159, 3254–3268.  
909 <https://doi.org/10.1016/j.envpol.2011.03.038>
- 910 del Grosso, S.J., Mosier, A.R., Parton, W.J., Ojima, D.S., 2005. DAYCENT model analysis of  
911 past and contemporary soil N<sub>2</sub>O and net greenhouse gas flux for major crops in the USA.  
912 *Soil Tillage Res* 83, 9–24. <https://doi.org/10.1016/J.STILL.2005.02.007>
- 913 del Grosso, S.J., Ogle, S.M., Nevison, C., Gurung, R., Parton, W.J., Wagner-Riddle, C., Smith,  
914 W., Winiwarter, W., Grant, B., Tenuta, M., Marx, E., Spencer, S., Williams, S., 2022. A  
915 gap in nitrous oxide emission reporting complicates long-term climate mitigation. *Proc*  
916 *Natl Acad Sci U S A* 119. <https://doi.org/10.1073/pnas.2200354119>
- 917 del Grosso, S.J., Ojima, D.S., Parton, W.J., Stehfest, E., Heistemann, M., DeAngelo, B., Rose,  
918 S., 2009. Global scale DAYCENT model analysis of greenhouse gas emissions and  
919 mitigation strategies for cropped soils. *Glob Planet Change* 67, 44–50.  
920 <https://doi.org/10.1016/J.GLOPLACHA.2008.12.006>
- 921 Erisman, J.W., Galloway, J., Seitzinger, S., Bleeker, A., Butterbach-Bahl, K., 2011. Reactive  
922 nitrogen in the environment and its effect on climate change. *Curr Opin Environ Sustain*  
923 3, 281–290. <https://doi.org/10.1016/J.COSUST.2011.08.012>
- 924 European Commission-Press release Nitrates: Commission decides to refer Greece to the  
925 Court of Justice and asks for financial sanctions, n.d.
- 926 European Soil Database (ESDB) v2.0 - raster version [WWW Document], n.d. URL  
927 [https://esdac.jrc.ec.europa.eu/ESDB\\_Archive/ESDB/ESDB\\_Data/ESDB\\_v2\\_data\\_smu\\_](https://esdac.jrc.ec.europa.eu/ESDB_Archive/ESDB/ESDB_Data/ESDB_v2_data_smu_1k.html)  
928 [1k.html](https://esdac.jrc.ec.europa.eu/ESDB_Archive/ESDB/ESDB_Data/ESDB_v2_data_smu_1k.html) (accessed 1.13.23).



- 929 Franke, J.A., Müller, C., Elliott, J., Ruane, A.C., Jägermeyr, J., Balkovic, J., Ciais, P., Dury, M.,  
930 Falloon, P.D., Folberth, C., François, L., Hank, T., Hoffmann, M., Izaurrealde, R.C.,  
931 Jacquemin, I., Jones, C., Khabarov, N., Koch, M., Li, M., Liu, W., Olin, S., Phillips, M.,  
932 Pugh, T.A.M., Reddy, A., Wang, X., Williams, K., Zabel, F., Moyer, E.J., 2020. The  
933 GGCM Phase 2 experiment: Global gridded crop model simulations under uniform  
934 changes in CO<sub>2</sub>, temperature, water, and nitrogen levels (protocol version 1.0). *Geosci*  
935 *Model Dev* 13, 2315–2336. <https://doi.org/10.5194/gmd-13-2315-2020>
- 936 Fuchs, K., Merbold, L., Buchmann, N., Bretscher, D., Brilli, L., Fitton, N., Topp, C.F.E., Klumpp,  
937 K., Lieffering, M., Martin, R., Newton, P.C.D., Rees, R.M., Rolinski, S., Smith, P., Snow,  
938 V., 2020. Multimodel Evaluation of Nitrous Oxide Emissions From an Intensively  
939 Managed Grassland. *J Geophys Res Biogeosci* 125.  
940 <https://doi.org/10.1029/2019JG005261>
- 941 Gabrielle, B., Laville, P., Hénault, C., Nicoulaud, B., Germon, J.C., 2006. Simulation of nitrous  
942 oxide emissions from wheat-cropped soils using CERES. *Nutr Cycl Agroecosyst* 74, 133–  
943 146. <https://doi.org/10.1007/s10705-005-5771-5>
- 944 Galloway, J.N., Leach, A.M., Bleeker, A., Erisman, J.W., 2013. A chronology of human  
945 understanding of the nitrogen cycle. *Philosophical Transactions of the Royal Society B:*  
946 *Biological Sciences*. <https://doi.org/10.1098/rstb.2013.0120>
- 947 García-Vila, M., Fereres, E., Mateos, L., Orgaz, F., Steduto, P., 2009. Deficit irrigation  
948 optimization of cotton with aquacrop. *Agron J* 101, 477–487.  
949 <https://doi.org/10.2134/agronj2008.0179s>
- 950 Garnett, T., Appleby, M.C., Balmford, A., Bateman, I.J., Benton, T.G., Bloomer, P., Burlingame,  
951 B., Dawkins, M., Dolan, L., Fraser, D., Herrero, M., Hoffmann, I., Smith, P., Thornton,  
952 P.K., Toulmin, C., Vermeulen, S.J., Godfray, H.C.J., 2013. Sustainable intensification in  
953 agriculture: Premises and policies. *Science* (1979).  
954 <https://doi.org/10.1126/science.1234485>
- 955 Geels, C., Andersen, H. v., Ambelas Skjøth, C., Christensen, J.H., Ellermann, T., Løfstrøm,  
956 P., Gyldenkerne, S., Brandt, J., Hansen, K.M., Frohn, L.M., Hertel, O., 2012. Improved



- 957 modelling of atmospheric ammonia over Denmark using the coupled modelling system  
958 DAMOS. *Biogeosciences* 9, 2625–2647. <https://doi.org/10.5194/bg-9-2625-2012>
- 959 Godfray, H.C.J., Beddington, J.R., Crute, I.R., Haddad, L., Lawrence, D., Muir, J.F., Pretty, J.,  
960 Robinson, S., Thomas, S.M., Toulmin, C., 2010. Food security: The challenge of feeding  
961 9 billion people. *Science* (1979). <https://doi.org/10.1126/science.1185383>
- 962 Grote, R., Lehmann, E., Brümmer, C., Brüggemann, N., Szarzynski, J., Kunstmann, H., 2009.  
963 Modelling and observation of biosphere–atmosphere interactions in natural savannah in  
964 Burkina Faso, West Africa. *Physics and Chemistry of the Earth, Parts A/B/C* 34, 251–260.  
965 <https://doi.org/10.1016/J.PCE.2008.05.003>
- 966 Gurung, R.B., Ogle, S.M., Breidt, F.J., Williams, S.A., Parton, W.J., 2020. Bayesian calibration  
967 of the DayCent ecosystem model to simulate soil organic carbon dynamics and reduce  
968 model uncertainty. *Geoderma* 376. <https://doi.org/10.1016/j.geoderma.2020.114529>
- 969 Haas, E., Carozzi, M., Massad, R.S., Butterbach-Bahl, K., Scheer, C., 2022. Long term impact  
970 of residue management on soil organic carbon stocks and nitrous oxide emissions from  
971 European croplands. *Science of The Total Environment* 836, 154932.  
972 <https://doi.org/10.1016/J.SCITOTENV.2022.154932>
- 973 Haas, E., Klatt, S., Fröhlich, A., Kraft, P., Werner, C., Kiese, R., Grote, R., Breuer, L.,  
974 Butterbach-Bahl, K., 2013. LandscapeDNDC: A process model for simulation of  
975 biosphere-atmosphere-hydrosphere exchange processes at site and regional scale.  
976 *Landsc Ecol* 28, 615–636. <https://doi.org/10.1007/s10980-012-9772-x>
- 977 He, W., Jiang, R., He, P., Yang, J., Zhou, W., Ma, J., Liu, Y., 2018. Estimating soil nitrogen  
978 balance at regional scale in China’s croplands from 1984 to 2014. *Agric Syst* 167, 125–  
979 135. <https://doi.org/10.1016/J.AGSY.2018.09.002>
- 980 Heinen, M., 2006. Application of a widely used denitrification model to Dutch data sets.  
981 *Geoderma* 133, 464–473. <https://doi.org/10.1016/J.GEODERMA.2005.08.011>
- 982 Hénault, C., Bizouard, F., Laville, P., Gabrielle, B., Nicoulaud, B., Germon, J.C., Cellier, P.,  
983 2005. Predicting in situ soil N<sub>2</sub>O emission using NOE algorithm and soil database. *Glob  
984 Chang Biol* 11, 115–127. <https://doi.org/10.1111/j.1365-2486.2004.00879.x>



- 985 Holst, J., Grote, R., Offermann, C., Ferrio, J.P., Gessler, A., Mayer, H., Rennenberg, H., 2010.  
986 Water fluxes within beech stands in complex terrain. *Int J Biometeorol* 54, 23–36.  
987 <https://doi.org/10.1007/s00484-009-0248-x>
- 988 Houska, T., Kraft, P., Liebermann, R., Klatt, S., Kraus, D., Haas, E., Santabarbara, I., Kiese,  
989 R., Butterbach-Bahl, K., Müller, C., Breuer, L., 2017. Rejecting hydro-biogeochemical  
990 model structures by multi-criteria evaluation. *Environmental Modelling and Software* 93,  
991 1–12. <https://doi.org/10.1016/j.envsoft.2017.03.005>
- 992 IFADATA [WWW Document], n.d. URL <http://ifadata.fertilizer.org/ucSearch.aspx> (accessed  
993 1.13.19).
- 994 Jägermeyr, J., Müller, C., Ruane, A.C., Elliott, J., Balkovic, J., Castillo, O., Faye, B., Foster, I.,  
995 Folberth, C., Franke, J.A., Fuchs, K., Guarin, J.R., Heinke, J., Hoogenboom, G., Iizumi,  
996 T., Jain, A.K., Kelly, D., Khabarov, N., Lange, S., Lin, T.S., Liu, W., Mialyk, O., Minoli, S.,  
997 Moyer, E.J., Okada, M., Phillips, M., Porter, C., Rabin, S.S., Scheer, C., Schneider, J.M.,  
998 Schyns, J.F., Skalsky, R., Smerald, A., Stella, T., Stephens, H., Webber, H., Zabel, F.,  
999 Rosenzweig, C., 2021. Climate impacts on global agriculture emerge earlier in new  
1000 generation of climate and crop models. *Nat Food* 2, 873–885.  
1001 <https://doi.org/10.1038/s43016-021-00400-y>
- 1002 Janz, B., Havermann, F., Lashermes, G., Zuazo, P., Engelsberger, F., Torabi, S.M.,  
1003 Butterbach-Bahl, K., 2022. Effects of crop residue incorporation and properties on  
1004 combined soil gaseous N<sub>2</sub>O, NO, and NH<sub>3</sub> emissions—A laboratory-based measurement  
1005 approach. *Science of The Total Environment* 807, 151051.  
1006 <https://doi.org/10.1016/J.SCITOTENV.2021.151051>
- 1007 Jones, C.M., Spor, A., Brennan, F.P., Breuil, M.C., Bru, D., Lemanceau, P., Griffiths, B., Hallin,  
1008 S., Philippot, L., 2014. Recently identified microbial guild mediates soil N<sub>2</sub>O sink capacity.  
1009 *Nat Clim Chang* 4, 801–805. <https://doi.org/10.1038/nclimate2301>
- 1010 Kalivas, D., Kollias, V., Kalivas, D.P., Kollias, V.J., 2001. Effects of soil, climate and cultivation  
1011 techniques on cotton yield in Central Greece, using different statistical methods 21.  
1012 <https://doi.org/10.1051/agro:2001110i>



- 1013 Kasper, M., Foldal, C., Kitzler, B., Haas, E., Strauss, P., Eder, A., Zechmeister-Boltenstern,  
1014 S., Amon, B., 2019. N<sub>2</sub>O emissions and NO<sub>3</sub><sup>-</sup> leaching from two contrasting regions in  
1015 Austria and influence of soil, crops and climate: a modelling approach. *Nutr Cycl*  
1016 *Agroecosyst* 113, 95–111. <https://doi.org/10.1007/s10705-018-9965-z>
- 1017 Kim, Y., Seo, Y., Kraus, D., Klatt, S., Haas, E., Tenhunen, J., Kiese, R., 2015. Estimation and  
1018 mitigation of N<sub>2</sub>O emission and nitrate leaching from intensive crop cultivation in the  
1019 Haean catchment, South Korea. *Science of The Total Environment* 529, 40–53.  
1020 <https://doi.org/10.1016/J.SCITOTENV.2015.04.098>
- 1021 Klatt, S., Kraus, D., Rahn, K.-H., Werner, C., Kiese, R., Butterbach-Bahl, K., Haas, E., 2015a.  
1022 Parameter-Induced Uncertainty Quantification of Regional N<sub>2</sub>O Emissions and NO<sub>3</sub><sup>-</sup>  
1023 Leaching using the Biogeochemical Model LandscapeDNDC . pp. 149–171.  
1024 <https://doi.org/10.2134/advagriconsystem6.2013.0001>
- 1025 Klatt, S., Kraus, D., Rahn, K.-H., Werner, C., Kiese, R., Butterbach-Bahl, K., Haas, E., 2015b.  
1026 Parameter-Induced Uncertainty Quantification of Regional N<sub>2</sub>O Emissions and NO<sub>3</sub><sup>-</sup>  
1027 Leaching using the Biogeochemical Model LandscapeDNDC . pp. 149–171.  
1028 <https://doi.org/10.2134/advagriconsystem6.2013.0001>
- 1029 Kraus, D., Weller, S., Klatt, S., Haas, E., Wassmann, R., Kiese, R., Butterbach-Bahl, K., 2014.  
1030 A new LandscapeDNDC biogeochemical module to predict CH<sub>4</sub> and N<sub>2</sub>O emissions from  
1031 lowland rice and upland cropping systems. *Plant Soil* 386, 125–149.  
1032 <https://doi.org/10.1007/s11104-014-2255-x>
- 1033 Larocque, G.R., Bhatti, J.S., Boutin, R., Chertov, O., 2008. Uncertainty analysis in carbon cycle  
1034 models of forest ecosystems: Research needs and development of a theoretical  
1035 framework to estimate error propagation. *Ecol Modell* 219, 400–412.  
1036 <https://doi.org/10.1016/J.ECOLMODEL.2008.07.024>
- 1037 Lee, K.M., Lee, M.H., Lee, J.S., Lee, J.Y., 2020. Uncertainty analysis of greenhouse gas  
1038 (GHG) emissions simulated by the parametric Monte Carlo simulation and nonparametric  
1039 bootstrap method. *Energies (Basel)* 13. <https://doi.org/10.3390/en13184965>



- 1040 Lehuger, S., Gabrielle, B., Oijen, M. van, Makowski, D., Germon, J.C., Morvan, T., Hénault,  
1041 C., 2009a. Bayesian calibration of the nitrous oxide emission module of an agro-  
1042 ecosystem model. *Agric Ecosyst Environ* 133, 208–222.  
1043 <https://doi.org/10.1016/j.agee.2009.04.022>
- 1044 Lehuger, S., Gabrielle, B., Oijen, M. van, Makowski, D., Germon, J.C., Morvan, T., Hénault,  
1045 C., 2009b. Bayesian calibration of the nitrous oxide emission module of an agro-  
1046 ecosystem model. *Agric Ecosyst Environ* 133, 208–222.  
1047 <https://doi.org/10.1016/J.AGEE.2009.04.022>
- 1048 Leip, A., Busto, M., Corazza, M., Bergamaschi, P., Koeble, R., Dechow, R., Monni, S., de  
1049 Vries, W., 2011. Estimation of N<sub>2</sub>O fluxes at the regional scale: Data, models, challenges.  
1050 *Curr Opin Environ Sustain*. <https://doi.org/10.1016/j.cosust.2011.07.002>
- 1051 Li, C.S., 2000. Modeling trace gas emissions from agricultural ecosystems.
- 1052 Li, X., Yeluripati, J., Jones, E.O., Uchida, Y., Hatano, R., 2015. Hierarchical Bayesian  
1053 calibration of nitrous oxide (N<sub>2</sub>O) and nitrogen monoxide (NO) flux module of an agro-  
1054 ecosystem model: ECOSSE. *Ecol Modell* 316, 14–27.  
1055 <https://doi.org/10.1016/J.ECOLMODEL.2015.07.020>
- 1056 Lu, X., 2020. A meta-analysis of the effects of crop residue return on crop yields and water use  
1057 efficiency. *PLoS One* 15. <https://doi.org/10.1371/journal.pone.0231740>
- 1058 Lugato, E., Bampa, F., Panagos, P., Montanarella, L., Jones, A., 2014. Potential carbon  
1059 sequestration of European arable soils estimated by modelling a comprehensive set of  
1060 management practices. *Glob Chang Biol* 20, 3557–3567.  
1061 <https://doi.org/10.1111/gcb.12551>
- 1062 Lugato, E., Leip, A., Jones, A., 2018. Mitigation potential of soil carbon management  
1063 overestimated by neglecting N<sub>2</sub>O emissions. *Nat Clim Chang* 8, 219–223.  
1064 <https://doi.org/10.1038/s41558-018-0087-z>
- 1065 Lyra, A., Loukas, A., 2021. Impacts of irrigation and nitrate fertilization scenarios on  
1066 groundwater resources quantity and quality of the Almyros Basin, Greece. *Water Supply*  
1067 21, 2748–2759. <https://doi.org/10.2166/ws.2021.097>



- 1068 Mavromatis, T., 2016. Spatial resolution effects on crop yield forecasts: An application to  
1069 rainfed wheat yield in north Greece with CERES-Wheat. *Agric Syst* 143, 38–48.  
1070 <https://doi.org/10.1016/j.agsy.2015.12.002>
- 1071 Molina-Herrera, S., Grote, R., Santabábara-Ruiz, I., Kraus, D., Klatt, S., Haas, E., Kiese, R.,  
1072 Butterbach-Bahl, K., 2015. Simulation of CO<sub>2</sub> fluxes in European forest ecosystems with  
1073 the coupled soil-vegetation process model “LandscapeDNDC.” *Forests* 6, 1779–1809.  
1074 <https://doi.org/10.3390/f6061779>
- 1075 Molina-Herrera, S., Haas, E., Grote, R., Kiese, R., Klatt, S., Kraus, D., Butterbach-Bahl, K.,  
1076 Kampffmeyer, T., Friedrich, R., Andreae, H., Loubet, B., Ammann, C., Horváth, L., Larsen,  
1077 K., Gruening, C., Frumau, A., Butterbach-Bahl, K., 2017. Importance of soil NO emissions  
1078 for the total atmospheric NO<sub>x</sub> budget of Saxony, Germany. *Atmos Environ* 152, 61–76.  
1079 <https://doi.org/10.1016/J.ATMOSENV.2016.12.022>
- 1080 Molina-Herrera, S., Haas, E., Klatt, S., Kraus, D., Augustin, J., Magliulo, V., Tallec, T., Ceschia,  
1081 E., Ammann, C., Loubet, B., Skiba, U., Jones, S., Brümmer, C., Butterbach-Bahl, K.,  
1082 Kiese, R., 2016. A modeling study on mitigation of N<sub>2</sub>O emissions and NO<sub>3</sub> leaching at  
1083 different agricultural sites across Europe using LandscapeDNDC. *Science of the Total*  
1084 *Environment* 553, 128–140. <https://doi.org/10.1016/j.scitotenv.2015.12.099>
- 1085 Morris, M.D., 1991. Factorial Sampling Plans for Preliminary Computational Experiments,  
1086 TECHNOMETRICS.
- 1087 Musacchio, A., Re, V., Mas-Pla, J., Sacchi, E., 2020. EU Nitrates Directive, from theory to  
1088 practice: Environmental effectiveness and influence of regional governance on its  
1089 performance. *Ambio* 49, 504–516. <https://doi.org/10.1007/s13280-019-01197-8>
- 1090 Myrriotis, V., Rees, R.M., Topp, C.F.E., Williams, M., 2018a. A systematic approach to  
1091 identifying key parameters and processes in agroecosystem models. *Ecol Modell* 368,  
1092 344–356. <https://doi.org/10.1016/j.ecolmodel.2017.12.009>
- 1093 Myrriotis, V., Williams, M., Rees, R.M., Topp, C.F.E., 2019. Estimating the soil N<sub>2</sub>O emission  
1094 intensity of croplands in northwest Europe. *Biogeosciences* 16, 1641–1655.  
1095 <https://doi.org/10.5194/bg-16-1641-2019>



- 1096 Myrgiotis, V., Williams, M., Topp, C.F.E., Rees, R.M., 2018b. Improving model prediction of  
1097 soil N<sub>2</sub>O emissions through Bayesian calibration. *Science of the Total Environment* 624,  
1098 1467–1477. <https://doi.org/10.1016/j.scitotenv.2017.12.202>
- 1099 OECD (2020), Nutrient balance (indicator) [WWW Document] URL  
1100 <https://data.oecd.org/agrland/nutrient-balance.htm> (accessed 2.16.20).
- 1101 Ogle, S.M., Paustian, K., n.d. Downloaded from [www.nrcresearchpress.com](http://www.nrcresearchpress.com), J. Soil. Sci.
- 1102 Parton, W.J., Hartman, M., Ojima, D., Schimel, D., 1998. DAYCENT and its land surface  
1103 submodel: description and testing. *Glob Planet Change* 19, 35–48.  
1104 [https://doi.org/10.1016/S0921-8181\(98\)00040-X](https://doi.org/10.1016/S0921-8181(98)00040-X)
- 1105 Petersen, K., Kraus, D., Calanca, P., Semenov, M.A., Butterbach-Bahl, K., Kiese, R., 2021.  
1106 Dynamic simulation of management events for assessing impacts of climate change on  
1107 pre-alpine grassland productivity. *European Journal of Agronomy* 128, 126306.  
1108 <https://doi.org/10.1016/J.EJA.2021.126306>
- 1109 Petersen, R.J., Blicher-Mathiesen, G., Rolighed, J., Andersen, H.E., Kronvang, B., 2021. Three  
1110 decades of regulation of agricultural nitrogen losses: Experiences from the Danish  
1111 Agricultural Monitoring Program. *Science of The Total Environment* 787, 147619.  
1112 <https://doi.org/10.1016/J.SCITOTENV.2021.147619>
- 1113 Portmann, F.T., Siebert, S., Döll, P., 2010. MIRCA2000-Global monthly irrigated and rainfed  
1114 crop areas around the year 2000: A new high-resolution data set for agricultural and  
1115 hydrological modeling. *Global Biogeochem Cycles* 24, n/a-n/a.  
1116 <https://doi.org/10.1029/2008gb003435>
- 1117 Rahn, K.H., Werner, C., Kiese, R., Haas, E., Butterbach-Bahl, K., 2012. Parameter-induced  
1118 uncertainty quantification of soil N<sub>2</sub>O, NO and CO<sub>2</sub> emission from Höglwald spruce  
1119 forest (Germany) using the LandscapeDNDC model. *Biogeosciences* 9, 3983–3998.  
1120 <https://doi.org/10.5194/bg-9-3983-2012>
- 1121 Ramanantenasoa, M.M.J., Gilliot, J.M., Mignolet, C., Bedos, C., Mathias, E., Eglin, T.,  
1122 Makowski, D., Générumont, S., 2018. A new framework to estimate spatio-temporal



- 1123 ammonia emissions due to nitrogen fertilization in France. *Science of The Total*  
1124 *Environment* 645, 205–219. <https://doi.org/10.1016/J.SCITOTENV.2018.06.202>
- 1125 Ranucci, S., Bertolini, T., Vitale, L., di Tommasi, P., Ottaiano, L., Oliva, M., Amato, U., Fierro,  
1126 A., Magliulo, V., 2011. The influence of management and environmental variables on soil  
1127 N<sub>2</sub>O emissions in a crop system in Southern Italy. *Plant Soil* 343, 83–96.  
1128 <https://doi.org/10.1007/s11104-010-0674-x>
- 1129 Ravishankara, A.R., Daniel, J.S., Portmann, R.W., 2009. Nitrous oxide (N<sub>2</sub>O): The dominant  
1130 ozone-depleting substance emitted in the 21st century. *Science* (1979) 326, 123–125.  
1131 <https://doi.org/10.1126/science.1176985>
- 1132 Refsgaard, J.C., van der Sluijs, J.P., Højberg, A.L., Vanrolleghem, P.A., 2007. Uncertainty in  
1133 the environmental modelling process – A framework and guidance. *Environmental*  
1134 *Modelling & Software* 22, 1543–1556. <https://doi.org/10.1016/J.ENVSOFT.2007.02.004>
- 1135 Robert, C., Casella, G., 2011. A short history of Markov Chain Monte Carlo: Subjective  
1136 recollections from incomplete data. *Statistical Science* 26, 102–115.  
1137 <https://doi.org/10.1214/10-STS351>
- 1138 Schroeck, A.M., Gaube, V., Haas, E., Winiwarter, W., 2019. Estimating nitrogen flows of  
1139 agricultural soils at a landscape level – A modelling study of the Upper Enns Valley, a  
1140 long-term socio-ecological research region in Austria. *Science of the Total Environment*  
1141 665, 275–289. <https://doi.org/10.1016/j.scitotenv.2019.02.071>
- 1142 SensitivityAnalysis, n.d.
- 1143 Sidiropoulos, C., Tsilingiridis, G., 2009. Trends of livestock-related NH<sub>3</sub>, CH<sub>4</sub>, N<sub>2</sub>O and PM  
1144 emissions in Greece. *Water Air Soil Pollut* 199, 277–289. [https://doi.org/10.1007/s11270-](https://doi.org/10.1007/s11270-008-9877-7)  
1145 [008-9877-7](https://doi.org/10.1007/s11270-008-9877-7)
- 1146 Smerald, A., Fuchs, K., Kraus, D., Butterbach-Bahl, K., Scheer, C., 2022. Significant Global  
1147 Yield-Gap Closing Is Possible Without Increasing the Intensity of Environmentally Harmful  
1148 Nitrogen Losses. *Front Sustain Food Syst* 6. <https://doi.org/10.3389/fsufs.2022.736394>
- 1149 Smith, P., Martino, D., Cai, Z., Gwary, D., Janzen, H., Kumar, P., McCarl, B., Ogle, S., O'Mara,  
1150 F., Rice, C., Scholes, B., Sirotenko, O., Howden, M., McAllister, T., Pan, G., Romanenkov,



- 1151 V., Schneider, U., Towprayoon, S., Wattenbach, M., Smith, J., 2008. Greenhouse gas  
1152 mitigation in agriculture. *Philosophical Transactions of the Royal Society B: Biological*  
1153 *Sciences*. <https://doi.org/10.1098/rstb.2007.2184>
- 1154 Stehfest, E., Bouwman, L., 2006. N<sub>2</sub>O and NO emission from agricultural fields and soils under  
1155 natural vegetation: Summarizing available measurement data and modeling of global  
1156 annual emissions. *Nutr Cycl Agroecosyst* 74, 207–228. [https://doi.org/10.1007/s10705-](https://doi.org/10.1007/s10705-006-9000-7)  
1157 [006-9000-7](https://doi.org/10.1007/s10705-006-9000-7)
- 1158 SUSTAINABLE AGRICULTURE IN EUROPE, 2009.
- 1159 Sutton, M.A., Reis, S., Riddick, S.N., Dragosits, U., Nemitz, E., Theobald, M.R., Tang, Y.S.,  
1160 Braban, C.F., Vieno, M., Dore, A.J., Mitchell, R.F., Wanless, S., Daunt, F., Fowler, D.,  
1161 Blackall, T.D., Milford, C., Flechard, C.R., Loubet, B., Massad, R., Cellier, P., Personne,  
1162 E., Coheur, P.F., Clarisse, L., van Damme, M., Ngadi, Y., Clerbaux, C., Skjøth, C.A.,  
1163 Geels, C., Hertel, O., Kruit, R.J.W., Pinder, R.W., Bash, J.O., Walker, J.T., Simpson, D.,  
1164 Horváth, L., Misselbrook, T.H., Bleeker, A., Dentener, F., de Vries, W., 2013. Towards a  
1165 climate-dependent paradigm of ammonia emission and deposition. *Philosophical*  
1166 *Transactions of the Royal Society B: Biological Sciences* 368.  
1167 <https://doi.org/10.1098/rstb.2013.0166>
- 1168 Thomas, D., Johannes, K., David, K., Rüdiger, G., Ralf, K., 2016. Impacts of management and  
1169 climate change on nitrate leaching in a forested karst area. *J Environ Manage* 165, 243–  
1170 252. <https://doi.org/10.1016/J.JENVMAN.2015.09.039>
- 1171 Thompson, R.L., Lassaletta, L., Patra, P.K., Wilson, C., Wells, K.C., Gressent, A., Koffi, E.N.,  
1172 Chipperfield, M.P., Winiwarter, W., Davidson, E.A., Tian, H., Canadell, J.G., 2019.  
1173 Acceleration of global N<sub>2</sub>O emissions seen from two decades of atmospheric inversion.  
1174 *Nat Clim Chang* 9, 993–998. <https://doi.org/10.1038/s41558-019-0613-7>
- 1175 Tracking progress towards Kyoto and 2020 targets in Europe — European Environment  
1176 Agency [WWW Document], n.d. URL [https://www.eea.europa.eu/publications/progress-](https://www.eea.europa.eu/publications/progress-towards-kyoto)  
1177 [towards-kyoto](https://www.eea.europa.eu/publications/progress-towards-kyoto) (accessed 1.13.19).



- 1178 Triantakonstantis, D., Detsikas, S., n.d. Applying Sustainable Agricultural Management  
1179 Practices in Saline and Sodic Soils to Increase Soil Organic Carbon Sequestration  
1180 Potential and Mitigate Climate Change.
- 1181 Tsakmakis, I.D., Kokkos, N.P., Gikas, G.D., Pisinaras, V., Hatzigiannakis, E., Arampatzis, G.,  
1182 Sylaios, G.K., 2019. Evaluation of AquaCrop model simulations of cotton growth under  
1183 deficit irrigation with an emphasis on root growth and water extraction patterns. *Agric  
1184 Water Manag* 213, 419–432. <https://doi.org/10.1016/j.agwat.2018.10.029>
- 1185 van Oijen, M., Rougier, J., Smith, R., 2005. Bayesian calibration of process-based forest  
1186 models: Bridging the gap between models and data, in: *Tree Physiology*. Oxford  
1187 University Press, pp. 915–927. <https://doi.org/10.1093/treephys/25.7.915>
- 1188 Velthof, G.L., Oudendag, D., Witzke, H.P., Asman, W.A.H., Klimont, Z., Oenema, O., 2009.  
1189 Integrated Assessment of Nitrogen Losses from Agriculture in EU-27 using MITERRA-  
1190 EUROPE. *J Environ Qual* 38, 402–417. <https://doi.org/10.2134/jeq2008.0108>
- 1191 Velthof, G.L., van Bruggen, C., Groenestein, C.M., de Haan, B.J., Hoogeveen, M.W.,  
1192 Huijsmans, J.F.M., 2012. A model for inventory of ammonia emissions from agriculture in  
1193 the Netherlands. *Atmos Environ* 46, 248–255.  
1194 <https://doi.org/10.1016/J.ATMOSENV.2011.09.075>
- 1195 Verbeeck, H., Samson, R., Verdonck, F., Lemeur, R., 2006. Parameter sensitivity and  
1196 uncertainty of the forest carbon flux model FORUG: A Monte Carlo analysis, in: *Tree  
1197 Physiology*. Oxford University Press, pp. 807–817.  
1198 <https://doi.org/10.1093/treephys/26.6.807>
- 1199 Vogeler, I., Giltrap, D., Cichota, R., 2013. Comparison of APSIM and DNDC simulations of  
1200 nitrogen transformations and N<sub>2</sub>O emissions. *Science of the Total Environment* 465,  
1201 147–155. <https://doi.org/10.1016/j.scitotenv.2012.09.021>
- 1202 Voloudakis, D., Karamanos, A., Economou, G., Kalivas, D., Vahamidis, P., Kotoulas, V.,  
1203 Kapsomenakis, J., Zerefos, C., 2015. Prediction of climate change impacts on cotton  
1204 yields in Greece under eight climatic models using the AquaCrop crop simulation model



1205 and discriminant function analysis. *Agric Water Manag* 147, 116–128.  
1206 <https://doi.org/10.1016/j.agwat.2014.07.028>  
1207 Wagner-Riddle, C., Congreves, K.A., Abalos, D., Berg, A.A., Brown, S.E., Ambadan, J.T., Gao,  
1208 X., Tenuta, M., 2017. Globally important nitrous oxide emissions from croplands induced  
1209 by freeze-thaw cycles. *Nat Geosci* 10, 279–283. <https://doi.org/10.1038/ngeo2907>  
1210 Wainwright, J., Mulligan, M., n.d. Environmental Modelling Finding Simplicity in Complexity  
1211 Editors.  
1212 Wang, G., Chen, S., 2012. A review on parameterization and uncertainty in modeling  
1213 greenhouse gas emissions from soil. *Geoderma* 170, 206–216.  
1214 <https://doi.org/10.1016/J.GEODERMA.2011.11.009>  
1215 Werner, C., Haas, E., Grote, R., Gauder, M., Graeff-Hönninger, S., Claupein, W., Butterbach-  
1216 Bahl, K., 2012. Biomass production potential from *Populus* short rotation systems in  
1217 Romania. *GCB Bioenergy* 4, 642–653. <https://doi.org/10.1111/j.1757-1707.2012.01180.x>  
1218 Yaalon, D.H., 1997. Soils in the Mediterranean region: what makes them different? *Catena*  
1219 (Amst) 28, 157–169. [https://doi.org/10.1016/S0341-8162\(96\)00035-5](https://doi.org/10.1016/S0341-8162(96)00035-5)  
1220 Zhang, W., Liu, C., Zheng, X., Zhou, Z., Cui, F., Zhu, B., Haas, E., Klatt, S., Butterbach-Bahl,  
1221 K., Kiese, R., 2015. Comparison of the DNDC, LandscapeDNDC and IAP-N-GAS models  
1222 for simulating nitrous oxide and nitric oxide emissions from the winter wheat–summer  
1223 maize rotation system. *Agric Syst* 140, 1–10.  
1224 <https://doi.org/10.1016/J.AGSY.2015.08.003>  
1225



1226 11 Appendix

1227 11.1 Material and Methods

1228 **Sensitivity Index**

1229 In the first step, the Sensitivity Index algorithm (SI) (Pannell, 1997) was calculated for all  
 1230 process parameters by splitting the parameter ranges into 10 equidistant values from minimum  
 1231 to maximum and by rating SI values:

$$1232 \quad SI = \frac{CUM_{max} - CUM_{min}}{CUM_{max}}$$

1233 where  $CUM_{max}$  and  $CUM_{min}$  are the maximum and minimum cumulative results of 10  
 1234 simulations. High SI values explain a high sensitivity of the underlying parameter with respect  
 1235 to the model results, whereas low values or even zero indicates low or no sensitivity.

1236

1237 11.2 Results

1238 *Table A 1. Observed yield rates in the region of Thessaly. Cotton yields are the cotton bolls, clover feed is the total*  
 1239 *harvested above ground biomass, for wheat and barley it is the grain yield, maize is accounted grain ear and the*  
 1240 *stems Source ELSTAT.*

Crop Yields [tons dry matter ha <sup>-1</sup> ]						
Crops	2012	2013	2014	2015	2016	Mean
Cotton	2.7	3.6	3.5	3.4	3.3	3.3
Clover	8.6	8.9	8.7	7.9	7.7	8.4
Wheat	3.3	3.3	3.3	3.7	3.6	3.4
Barley	3.2	3.2	3.2	3.5	3.5	3.3
Maize	10.9	12.1	12.3	12.7	12.1	12.0

1241

1242 *Table A 2. Crop rotation scenarios (R1 – R5) for the region of Thessaly where the crop abbreviations corn, wiwh,*  
 1243 *perg, cott and wbar refer to maize, winter wheat, clover (legume feed crops s.a. alfalfa or vetch), cotton and winter*  
 1244 *barley respectively.*

years	R1	R2	R3	R4	R5
2010	corn	wiwh	perg	cott	wbar
2011	wiwh	perg	cott	wbar	corn
2012	perg	cott	wbar	corn	wiwh
2013	cott	wbar	corn	wiwh	perg



2014	wbar	corn	wiwh	perg	cott
2015	corn	wiwh	perg	cott	wbar
2016	wiwh	perg	cott	wbar	corn

1245

1246 *Table A 3. Carbon Balance (totals) Summary of the Assessment and Uncertainty Analysis of the of cropland*  
 1247 *cultivation of the region of Thessaly, Greece, GPP gross primary productivity, TER terrestrial ecosystem respiration,*  
 1248 *Biomass export includes all C in yield, straw and feed exported from the fields, 360000 ha cropland.*

	Mean	Std	Median	Q25	Q75
	[mio. tons C yr <sup>-1</sup> ]				
C-Inputs	4.51	0.20	4.45	4.36	4.69
C-Outputs	4.32	0.17	4.31	4.19	4.45
SOC-changes	0.19	0.11	0.20	0.14	0.27
Input fluxes					
GPP	4.25	0.20	4.21	4.11	4.42
C in manure	0.25	0.01	0.26	0.25	0.26
Output fluxes					
TER	3.08	0.16	3.06	2.97	3.20
Biomass export	1.24	0.05	1.24	1.21	1.27

1249

1250 *Table A 4 Nitrogen balance (totals) Summary of the Assessment and Uncertainty Analysis of the total Nitrogen*  
 1251 *Balance of cropland cultivation of the region of Thessaly, Greece.*

	Mean	Std	Median	Q25	Q75
	[kt-N yr <sup>-1</sup> ]				
N-Inputs	76.5	3.2	77.8	73.3	79.1
N-Outputs	71.7	3.2	71.2	69.4	73.7
N-stock-changes	4.8	0.0	6.6	3.9	5.4
Input fluxes					
N deposition	2.0	0.3	2.1	1.9	2.1
Bio. N fixation	16.7	1.6	16.7	15.9	17.5
N in min. fertilizer	28.9	1.7	29.3	27.6	29.8
N in organic fertilizer	28.9	1.3	29.2	27.9	29.8



Output fluxes					
Gaseous emissions <sup>1)</sup>	21.2	3.1	21.1	18.9	23.4
N <sub>2</sub> O	0.9	0.3	0.9	0.7	1.1
NO	1.1	0.5	1.0	0.7	1.4
N <sub>2</sub>	4.9	2.4	4.5	2.9	6.6
NH <sub>3</sub>	14.3	2.6	13.5	12.5	15.6
Aquatic fluxes <sup>2)</sup>					
NO <sub>3</sub> leaching	3.9	1.3	3.8	3.0	4.7

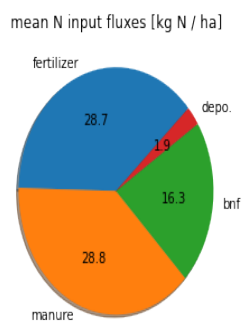
1252 1) Gaseous emissions are the sum of N<sub>2</sub>O, NO, N<sub>2</sub> and NH<sub>3</sub> fluxes; 2) Aquatic flux is nitrate leaching (NO<sub>3</sub>-)

1253

1254 Table A 5. Total crop yields per cultivar and year.

Crop Yields [tons dry matter]						
Crops	2012	2013	2014	2015	2016	Mean
Cotton	303 676.9	374 424.6	359 806.7	322 292.0	285 780.3	329 196.1
Clover	302 753.2	319 401.7	338 134.6	341 938.4	360 693.9	332 584.4
Wheat	477 700.7	461 875.5	395 902.1	430 014.4	450 254.3	443 149.4
Barley	84 520.8	99 091.8	139 402.9	139 990.8	102 454.7	113 092.2
Maize	332 531.6	431 324.6	377 783.9	351 285.4	334 277.7	365 440.6

1255



1256

1257 Figure 9. Shares of components of the annual nitrogen in- and output fluxes.

1258

1259 Table A 6. Simulated crop yields per cultivar and year for the irrigated land.

Crop Yields [tons dry matter ha <sup>-1</sup> ]
---



Crops	Median	Mean	STD
Cotton	4.0	3.7	0.9
Clover	9.8	9.6	0.6
Wheat	3.9	3.6	0.9
Barley	5.3	5.0	1.2
Maize	10.9	10.6	1.3

1260

1261 *Table A 7. Simulated crop yields per cultivar and year for the rain feed land.*

Crop Yields [tons dry matter ha <sup>-1</sup> ]			
Crops	Median	Mean	STD
Cotton	3.0	2.9	0.7
Clover	9.8	9.6	0.6
Wheat	3.9	3.6	0.9
Barley	4.0	3.9	0.9
Maize	9.5	9.2	1.5

1262